Acoustic Propagation and Scattering through the Lined Cavities

by

Hafiza Umara Ismail

A thesis submitted in partial fulfillment for the
degree of Master of Philosophy

in the
Faculty of Computing
Department of Mathematics

2020

This thesis is dedicated to my beloved parents for their love, endless support, encouragement and for their guidance.

CERTIFICATE OF APPROVAL

Acoustic Propagation and Scattering through the Lined Cavities

by

Hafiza Umara Ismail

(MMT173001)

THESIS EXAMINING COMMITTEE

S. No.	Examiner	Name	Organization
(a)	External Examiner	Dr. Abdul Wahab	NUST, Islamabad
(b)	Internal Examiner	Dr. Abdul Rehman Kashif	CUST, Islamabad
(c)	Supervisor	Dr. Muhammad Afzal	CUST, Islamabad

Dr. Muhammad Afzal
Thesis Supervisor
August, 2020

Dr. Muhammad Sagheer
Head
Dept. of Mathematics
August, 2020

Dr. Muhammad Abdul Qadir
Dean
Faculty of Computing
August, 2020

Author's Declaration

I, **Hafiza Umara Ismail** hereby state that my M.Phil thesis titled "**Acoustic Propagation and Scattering through the Lined Cavities**" is my own work and has not been submitted previously by me for taking any degree from Capital University of Science and Technology, Islamabad or anywhere else in the country/abroad.

At any time if my statement is found to be incorrect even after my graduation, the University has the right to withdraw my M.Phil Degree.

(Hafiza Umara Ismail)

Registration No: MMT173001

Plagiarism Undertaking

I solemnly declare that research work presented in this thesis titled "**Acoustic Propagation and Scattering through the Lined Cavities**" is solely my research work with no significant contribution from any other person. Small contribution/help wherever taken has been dully acknowledged and that complete thesis has been written by me.

I understand the zero tolerance policy of the HEC and Capital University of Science and Technology towards plagiarism. Therefore, I as an author of the above titled thesis declare that no portion of my thesis has been plagiarized and any material used as reference is properly referred/cited.

I undertake that if I am found guilty of any formal plagiarism in the above titled thesis even after award of M.Phil Degree, the University reserves the right to withdraw/revoke my M.Phil degree and that HEC and the University have the right to publish my name on the HEC/University website on which names of students are placed who submitted plagiarized work.

(Hafiza Umara Ismail)

Registration No: MMT173001

Acknowledgements

In the name of **ALLAH**, the most Beneficent, the most Merciful. It was not possible to complete this thesis without faith in Allah, who made me to stay strong and patient until the end. All great abundant thanks to the Glorious Almighty Allah, for all his blessing on me throughout my life and who enable me to complete my thesis work.

I am deeply obliged to my supervisor **Dr. Muhammad Afzal** who guided me alot in my research work and spending many hours discussing and reviewing of this thesis. The preparation of this thesis would never have been possible without his constructive suggestions and encouragement. His keen interest and valuable suggestions made this work to end.

I am also deeply indebted to my respected **HOD**, **Dr. Muhammad Sagheer** and my all respected teachers in the Department of Mathematics, Capital University of Science and Technology.

I want to pay special thanks to my father Muhammad Ismail and sister Uniza Ismail who helped me alot in this work. I acknowledge the co-operation of Madam Rukayya for her support and well wishes. I am also thankful to my best friends Nadia and Sadia who helped me alot during this work directly or indirectly.

Finally i would like to thanks my brothers for their love and best wishes.

(Hafiza Umara Ismail)

Registration No: MMT173001

Abstract

In the present work the reflection and transmission through the chamber cavities including liners are analyzed. To explain the mechanism of Multi-modal technique two prototype problems are discussed. These physical problems include rigid-rigid and rigid-impedance type boundary conditions and are radiated by a plane piston. The governing boundary value problems are solved via Multi-modal and Mode-matching techniques. It is found that by changing the velocity of the piston a variation in scattering amplitudes is found. Moreover, there exists an excellent agreement between the Multi-modal and Mode-matching results. Furthermore, a physical problem including liner cavities in the expansion chamber is formulated, and is solved by using the Multi-modal approach. The envisaged problem comprises excitation from the inlet and the transmission from the outlet after interaction with liner cavities. The inlet region also contain reflection of radiated waves. The absolute value of fundamental reflected and transmitted mode amplitudes are plotted against frequency. It is found that by changing the depth and length of the chamber cavities a variation in passing and stopping bands in found.

Contents

List of Figures

Chapter 1

Introduction

Acoustic liners [1] are used to reduce the noise emitting from Heating Ventilation and Air Conditioning (HVAC) systems of buildings, chimney stacks, power stations, vehicles and aeroplanes. The frequently used acoustic liners are bulk reacting liners and locally reacting liners. Generally the locally reacting liners are constructed by the perforated sheet of honeycomb layers that allow the propagation of waves normal to the duct wall. Locally reacting liners have the good absorption quality for small frequency range of noises. The main control of these liners are their validity and high potential of resistance. On the other hand, bulk reacting liners have broad absorption quality. These liners are composed of porous material and show less efficiency at lower frequency regime as compared with locally reacting liners. To control the low frequency range of noises, is infact a challenging issue.

The current work is related to the reflection and transmission of acoustic waves in the channel containing reacting liners. The Multi-modal scheme is adopted to analyze the scattering behavior of incoming propagative modes in the presence of locally reacting liners. The propagation of modes is linked with the eigenvalues and eigenvectors of transformed system. To ensure the accuracy of collected modes two simple duct problems are considered. First problem is bounded by rigid walls and is excited with a plane piston along the wall, whereas, in the later problem the upper rigid wall is replaced with impedance surface. Both of these problems are

solved with Multi-modal and Mode-matching schemes. To confirm the accuracy of Multi-modal method the model coefficients are compared for different velocities of moving piston. The worked is stated comprehensively in Chapter 3. However the modeling of locally reacting liners of the cavities is discussed in Chapter 4. By considering the locally reacting liners as a component of reactive silencer the Multi-modal scheme is developed.

1.1 Literature Review and Background

Propagation of sound waves in lined ducts having rigid walls have been discussed by many authors for instance see [2]-[3]. Various methods were preferred to study the propagation of sound waves in duct lined with locally reacting liners by using impedance condition. These methods include; Mode-matching method [4], Finite element method [5] and Point matching method [6]. Each approach has strength and limitation depending upon the considered model and the aims of investigations. Felix [7] assumed adiabatic lossy medium lined with reacting liners. In his paper he considered the circular curved duct system and with the aid of Multi-modal approach the velocity and pressure components are calculated by using impedance conditions.

Likewise, Pagneux and Auregan [8] assumed a circular rigid duct lined with a non-uniform reacting liners. The impedance condition assumed to be piece-wise constant across the duct boundary and the Multi-modal method was used to sort the solution of the problem. They found that duct modes with rigid walls are linked with the eigenvalues and eigenfunctions of transformed system. The method fits well to analyze the vibrations having low, mid and high frequencies. The numerical results showed that the non-uniform liners have minor effects on the efficiency of the devise.

Kirby [9] considered two different silencers of an exhaust system radiated from inlet pipe. He equiped the device with reactive and dissipative tools and concluded that the acoustic behavior of energy in silencers can be improved for higher frequency

modes by reactive and dissipative materials. The Mode-matching technique has been used by many researchers to analyze the scattering of energy in active and passive liners for instance, see [10–20]. The present thesis focuses on the scattering of acoustic waves in reactive chamber silencer containing acoustic reacting liners. The Multi-modal method is applied here to find the solution of physical problems.

To confirm the accuracy of performed scheme first two prototype problems are discussed by using of Multi-modal and Mode-matching schemes. Result obtained by these schemes are compared in Chapter 3. However in Chapter 4 only the Multi-modal solution is presented. The thesis is organized as follows. Chapter 3 contain basic transformation. In Chapter 4 scattering of acoustic waves has been discussed in a rigid duct having three channels, in which central part of the duct is lined through locally reacting liners. The eigen functions satisfy the orthogonality relation. The transmission and reflection coefficients are then calculated. The results and consequences are discussed at the end of the each Chapter.

Chapter 2

Preliminaries

This thesis contains physical problems that are relevant to the reflection, transmission and absorption of acoustic waves propagating in rectangular ducts or channels. The purpose of present chapter is to discuss some basic terminologies which are useful in understanding the mathematical modeling and associated physical characteristics of the work presented in rest of the chapters.

2.1 What is Wave?

Wave is the disturbance in the medium which causes the particles of that medium to vibrate from one place to another to transfer the energy. It is important to know that waves transfer energy of the matter without transferring matter. Typical examples include light waves and sound waves etc.

2.2 Types of Waves

There are three types of waves based on the medium characteristics and energy propagation. These types include:

1) Mechanical waves.

2) Electromagnetic waves.

3) Matter waves.

2.2.1 Mechanical Waves

Mechanical waves are the type of waves in which energy is transferred through the oscillations produced in a material medium. Waves produced on the strings and springs, waves produce on the water surface are some common examples. Mechanical waves are classified into longitudinal waves and transverse waves depending upon their direction of motion of propagating waves and the vibration of the particles of medium.

Longitudinal Waves

Longitudinal waves are the waves in which direction of particles of medium are parallel to the direction of propagation of waves. Sound waves and pressure waves are some common examples of longitudinal waves.

Transverse Waves

If the direction of particles of medium are perpendicular to the direction of propagating waves then this type of waves are known as transverse waves. Examples of transverse waves are waves produce on slinky spring, electromagnetic waves.

2.2.2 Electromagnetic Waves

The waves which are created when electric and magnetic fields oscillate perpendicular to each other are known as electromagnetic waves. These are the only waves that do not need any material medium for the transfer of energy. These waves travel in a vacuum with the same speed. The X rays, microwaves and radiowaves are some common examples of electromagnetic waves.

2.2.3 Matter Waves

Light has both the natures, sometimes it act as radiation and sometimes it acts as material which has momentum and which can strike with a force. The dual nature of light to exist as both material and in wave form is known as matter waves.

2.3 Properties of Waves

For further explanation about waves, it is appropriate to know about basic properties of waves.

Time Period

The time taken by a vibrating body to complete one vibration is called time period. It is denoted as T.

Frequency

The number of vibrations of a vibrating body completed in unit time is called its frequency. It is represented as f and is measured in Hertz (Hz).

Amplitude

The maximum displacement of vibrating body from its mean position is called amplitude.

Wavelength

The distance between two consecutive crests or troughs is called the wavelength of the wave. It is represented as λ.

Crest

The crest is the highest point of the particles of the wave in a medium from mean position.

Trough

The lowest point of the particles of vibrating body from the mean position is called trough.

Compression

The region in the medium in which the particles of the medium are close together is called compression.

Rarefaction

The region of the vibrating body where the particles of the medium are far apart from each other is known as rarefaction.

2.4 Acoustics

Acoustics is the branch of science which deals with the propagation of mechanical waves in matter. This branch covers how sound energy emits, reflects and transmits through a medium. The term acoustics is derived from Greek word akoustikos which means to hear. Normal human frequency range of hearing lies between 20 Hz to 20k Hz. The vibrations with frequency less than 20 Hz is known as infra sound and above than 20k Hz is ultra sound.

2.5 Acoustic Wave Equation

The acoustic wave equation in terms of sound pressure can be derived on the basis of following principles.

- Conservation of mass:
$$\frac{\partial \rho}{\partial t} + \nabla \cdot (\rho \mathbf{u}) = 0. \tag{2.1}$$

- Conservation of momentum:

$$\rho \left(\frac{\partial \mathbf{u}}{\partial t} + (\mathbf{u} \cdot \nabla)\mathbf{u} \right) = -\nabla p + \rho g. \tag{2.2}$$

- Equation of state by assuming the process is adiabatic:

$$P = \beta s, \tag{2.3}$$

where acoustic pressure P can be expressed in terms of pressure perturbation form as

$$P = p - p_0 \tag{2.4}$$

and condensation s in terms of density variation is represented as follows

$$s = \frac{\rho - \rho_0}{\rho_0}. \tag{2.5}$$

On using (2.5) into (2.1), we get

$$\frac{\partial s}{\partial t} + \nabla \cdot \mathbf{u} = 0, \tag{2.6}$$

which is known as linear continuity equation. Also, on using (2.4) with assuming the dominant terms, we obtain linear Euler's equation.

$$\rho_0 \frac{\partial \mathbf{u}}{\partial t} = -\nabla P. \tag{2.7}$$

On taking gradient of (2.7), which yields

$$\nabla \cdot \rho_0 \left(\frac{\partial \mathbf{u}}{\partial t} \right) = -\nabla^2 P. \tag{2.8}$$

Now by taking time derivative of (2.8), we get

$$\rho_0 \frac{\partial^2 s}{\partial t^2} = -\nabla \left(\rho_0 \frac{\partial \mathbf{u}}{\partial t} \right). \tag{2.9}$$

On comparing equation (2.8) and (2.9), we get

$$\rho_0 \frac{\partial^2 s}{\partial t^2} = \nabla^2 P. \tag{2.10}$$

On using (2.3) into (2.10), that provides

$$\frac{1}{c^2} \frac{\partial^2 P}{\partial t^2} = \nabla^2 P \tag{2.11}$$

where $c = \sqrt{\frac{\beta}{\rho_0}}$ is the speed of sound. Now the acoustic pressure and velocity in terms of field potential form $\bar{\phi}(\bar{x}, \bar{y}, \bar{t})$ can be expressed as

$$P = -\rho_0 \frac{\partial \bar{\phi}}{\partial t} \quad \text{and} \quad u = \nabla \bar{\phi}. \tag{2.12}$$

Hence we can write (2.12) in terms dimensional field potential $\bar{\phi}(\bar{x}, \bar{y}, \bar{t})$, that is

$$\frac{1}{c^2} \frac{\partial^2 \bar{\phi}}{\partial t^2} = \nabla^2 \bar{\phi}. \tag{2.13}$$

On using the transformations $x = k\bar{x}$, $y = k\bar{y}$ and $t = \omega^{-1}\bar{t}$ with harmonic time dependence $e^{-i\omega t}$, we will get the dimensionless field potential ϕ that satisfies Helmholtz's equation, that is

$$\left(\nabla^2 + 1 \right) \phi = 0. \tag{2.14}$$

Chapter 3

Acoustic Propagation in Ducts Radiated by Plane Pistons

In this chapter the propagation of acoustic waves radiated by plane piston lying along the vertical wall of duct is discussed. The boundary conditions of horizontal walls are assumed to be rigid-rigid, rigid-impedance. The Multi-modal procedure is adopted to determine the propagating modes in the duct region, which are then compared with the eigen modes found through the separation of variable method to verify the results. The boundary value problem involve Helmholtz's equation in accompanying with impedance and rigid type boundary conditions. The mathematical formulation of waveguides is comprehensively discussed in each problem to obtained the desired results. The solution methodologies includes velocity condition. The numerical results are discussed at the end of the chapter.

3.1   Mathematical Formulation

Here we assume the wave propagation in two dimensional rectangular duct having boundaries at $y = 0$ and $y = h$ in xy-coordinates. The inside of the duct is filled with compressible fluid of density ρ and sound speed c. The physical configuration of the duct is as shown in Figure 3.1.
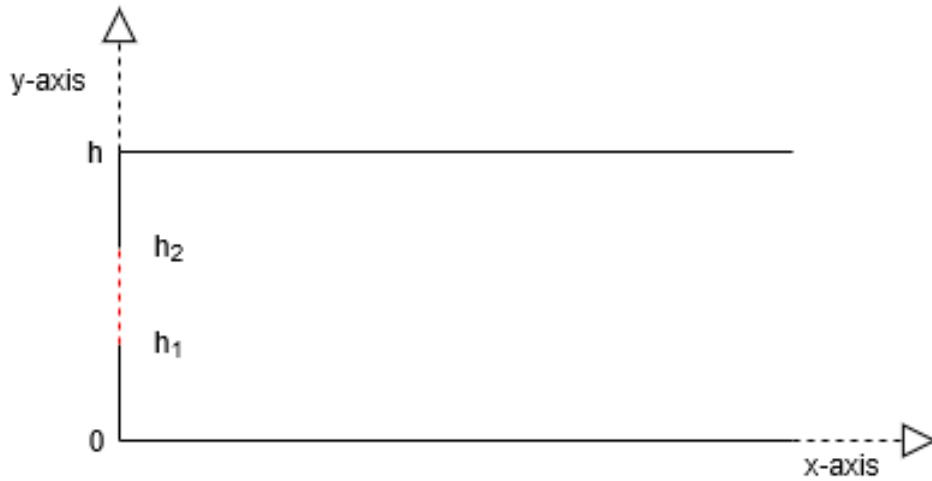
Figure 3.1: The geometry of the physical configuration of duct

The wave propagation in the duct can be characterized by the wave equation

$$\left\{\frac{\partial^2}{\partial x^2} + \frac{\partial^2}{\partial y^2}\right\} \Phi(x,y,t) = \frac{1}{c^2}\frac{\partial^2 \Phi}{\partial t^2} \tag{3.1}$$

where $\Phi(x,y,t)$ is the time dependent field potential. The acoustic pressure and normal velocity vector are related to the field potential by the relations

$$p = -\rho\frac{\partial \Phi}{\partial t} \tag{3.2}$$

and

$$\boldsymbol{v} = \triangledown\Phi, \tag{3.3}$$

respectively. Assuming the harmonic time dependence $e^{-i\omega t}$ in which ω is radiant frequency, we write

$$\Phi(x,y,t) = \phi(x,y)e^{-i\omega t}, \tag{3.4}$$

where $\phi(x,y)$ is the time independent field potential. By using (3.4) into (3.1,) we found

$$\left\{\frac{\partial^2}{\partial x^2} + \frac{\partial^2}{\partial y^2} + k^2\right\} \phi(x,y) = 0, \tag{3.5}$$

where $k = \omega/c$ is the wave number. The boundary conditions of the duct are assumed to contain two categories. These are explain in accompanying sub-sections.

3.2 Rigid-Rigid

First we assume a semi-infinite duct radiated by plane piston at $x = 0$. All the boundaries of semi-infinite duct are taken acoustically rigid. The physical configuration of the duct is shown in Figure 3.2.

Figure 3.2: The physical configuration of semi-infinite duct

For acoustically rigid boundaries, the normal velocity is zero, that is

$$\frac{\partial \phi}{\partial y} = 0, \quad y = 0, \quad 0 < x < \infty, \tag{3.6}$$

$$\frac{\partial \phi}{\partial y} = 0, \quad y = h, \quad 0 < x < \infty, \tag{3.7}$$

$$\frac{\partial \phi}{\partial x} = 0, \quad x = 0, \quad 0 < y < h_1, \tag{3.8}$$

$$\frac{\partial \phi}{\partial x} = 0, \quad x = 0, \quad h_1 < y < h. \tag{3.9}$$

Consider the duct is radiated with a plane piston lying along vertical wall $h_1 \leq y \leq h_2$ at $x = 0$, moving with constant velocity U. The velocity condition at $x = 0$ can be stated as

$$\frac{\partial \phi}{\partial x} = \begin{cases} 0, & 0 \leq y < h_1 \\ U, & h_1 \leq y \leq h_2 \\ 0, & h_2 < y \leq h \end{cases} . \tag{3.10}$$

The propagating waveforms in the duct region is determined by Mode-matching technique and Multi-modal technique. Both are discussed in the next sub-section.

• **Mode-matching Solution**

Here we apply the separation of variable technique to determine wave formulation of propagating modes. For this we let

$$\phi(x, y) = X(x)Y(y), \tag{3.11}$$

which on using into (3.5) leads to

$$\frac{Y''}{Y} + k^2 = -\frac{X''}{X} = \eta^2 \quad \text{(say)}. \tag{3.12}$$

On solving (3.12), we obtain

$$X(x) = c_1 e^{i\eta x} + c_2 e^{-i\eta x}, \tag{3.13}$$

and

$$Y(y) = c_3 \cos \tau y + c_4 \sin \tau y, \tag{3.14}$$

where $\tau = \sqrt{k^2 - \eta^2}$ and $c_1 - c_4$ are arbitrary constants. By using boundary conditions (3.6)-(3.7), we found $c_4 = 0$ and for non trivial form of solution

$$\sin(\tau h) = 0.$$

It reveals eigenvalues $\tau = \tau_n = n\pi/h$; $n = 0, 1, 2, ...$ and the eigenfunction $Y_n = \cos(\tau_n y)$, $n = 0, 1, 2, ...$These eigenfunctions are orthogonal in nature and satisfy

$$\int_0^h Y_m(y)Y_n(y) = 0, \quad \text{when} \quad m \neq n, \tag{3.15}$$

$$\int_0^h Y_m(y)Y_n(y) = h, \quad \text{when} \quad m = n = 0, \tag{3.16}$$

and

$$\int_0^h Y_m(y)Y_n(y) = \frac{h}{2}, \quad \text{when} \quad m = n \neq 0. \tag{3.17}$$

We can combine (3.15) to (3.17) to get the orthonormal relation

$$\int_0^h \psi_m(y)\psi_n(y)dy = \delta_{mn}, \tag{3.18}$$

where

$$\delta_{mn} = \begin{cases} 1 & m = n \\ 0 & m \neq 0 \end{cases}.$$

The orthonormal function $\psi_m(y)$ defined by

$$\psi_m = \Lambda_m \cos(\tau_m y), \tag{3.19}$$

in which

$$\Lambda_m = \begin{cases} \frac{1}{\sqrt{h}}, & m = 0, \\ \sqrt{\frac{2}{h}}, & m \geq 1. \end{cases} \tag{3.20}$$

Therefore, the propagating wave in positive $x-$direction can be given as

$$\phi(x,y) = \sum_{n=0}^{\infty} A_n \psi_n(y)e^{i\eta_n x}, \tag{3.21}$$

where $\eta_n = \sqrt{k^2 - \tau_n^2}$, is the nth mode wave number propagating in positive direction and A_n is the amplitude of nth mode which is unknown. To determine A_n, we match the normal velocity modes with executing modes at $x = 0$. Thus, on using (3.21) into (3.10), we obtain

$$i\sum_{n=0}^{\infty} A_n \psi_n(y)\eta_n = \begin{cases} 0, & 0 \leq y < h_1 \\ U, & h_1 \leq y \leq h_2 \\ 0, & h_2 < y \leq h \end{cases}. \tag{3.22}$$

On multiplying (3.22) with $\psi_m(y)$ and integrating from 0 to h, we get

$$i\sum_{m=0}^{\infty} A_n\eta_n \int_0^h \psi_n(y)\psi_m(y)dy = U\int_{h_1}^{h_2} \psi_m(y)dy. \tag{3.23}$$

By invoking orthonormal relation (3.18), (3.23) leads to

$$\sum_{m=0}^{\infty} A_n\eta_n\delta_{mn} = -iU\int_{h_1}^{h_2} \psi_m(y)dy \tag{3.24}$$

or

$$A_m = \frac{-iU}{\eta_m}Q_m, \tag{3.25}$$

where

$$Q_m = \int_{h_1}^{h_2} \psi_m(y)dy$$
$$= \begin{cases} \frac{h_2-h_1}{\sqrt{h}}, & m=0, \\ \sqrt{\frac{2}{h}}\frac{2}{m\pi}\left\{\sin(\frac{h_2\pi}{h}) - \sin(\frac{h_1\pi}{h})\right\}, & m \geq 1. \end{cases} \tag{3.26}$$

• Multi-modal Approach

Now we formulate the travelling waveforms by using the Multi-modal approach. For this, we assume the insatz

$$\phi(x,y) = \sum_{n=0}^{\infty} A_n Z_n(y)e^{is_nx}. \tag{3.27}$$

By using (3.27) into (3.5) and invoking the boundary conditions (3.6)-(3.7), we respectively found

$$\frac{d^2 Z_n}{dy^2} + \gamma_n^2 Z_n = 0 \tag{3.28}$$

and

$$Z_n'(0) = 0 \tag{3.29}$$

$$Z_n'(h) = 0 \tag{3.30}$$

where $\gamma_n^2 = \sqrt{k^2 - s_n^2}$ and prime shows the differentiation with respect to involved variable. Note that in (3.27), A_n, Z_n and s_n are unknowns. To determine these unknowns we establish here the associated eigenvalue problem.

● **Eigenvalue Problem**

$$\frac{d^2\xi_n(y)}{dy^2} + \alpha_n^2\xi_n(y) = 0, \tag{3.31}$$

$$\xi_n'(0) = 0, \tag{3.32}$$

$$\xi_n'(h) = 0. \tag{3.33}$$

By solving (3.31) with the aid of (3.32) and (3.33), we get the orthonormal form of $\xi_n(y)$ as

$$\xi_n = \Lambda_n \cos(\alpha_n y) \tag{3.34}$$

where

$$\alpha_n = \frac{n\pi}{h}, \tag{3.35}$$

and

$$\int_0^h \xi_n(y)\xi_m(y) = \delta_{mn}. \tag{3.36}$$

Let us assume $Z_n(y)$ as the linear combination of ξ_m as

$$Z_n(y) = \sum_{m=0}^{\infty} B_{nm}\xi_{nm}(y) = \boldsymbol{\xi}_n^t \boldsymbol{B}_n \tag{3.37}$$

where

$$\boldsymbol{\xi}_n^t = \begin{bmatrix} \xi_{n0} & \xi_{n1} & \cdots & \xi_{nm} & \cdots \end{bmatrix}, \tag{3.38}$$

and

$$\boldsymbol{B}_n^t = \begin{bmatrix} B_{n0} & B_{n1} & \cdots & B_{nm} & \cdots \end{bmatrix}. \tag{3.39}$$

Note that super script t denotes the transpose of a vector. On multiplying (3.28) with $\boldsymbol{\xi}_n$ and integrating over y from 0 to h, we get

$$\int_0^h \boldsymbol{\xi}_n \frac{d^2 Z_n}{dy^2} dy + \gamma_n^2 \int_0^h \boldsymbol{\xi}_n Z_n dy = 0. \tag{3.40}$$

On performing the integration by parts, the first term on the left hand side of (3.40) can be written as

$$\int_0^h \boldsymbol{\xi}_n \frac{d^2 Z_n}{dy^2} dy = \left(\boldsymbol{\xi}_n(y) \frac{dZ_n}{dy} \right) \Big|_0^h - \left(\frac{d\boldsymbol{\xi}_n}{dy} Z_n \right) \Big|_0^h + \int_0^h Z_n \frac{d^2 \boldsymbol{\xi}_n}{dy^2} dy. \qquad (3.41)$$

By substituting the boundary conditions (3.29)-(3.30) and (3.32)-(3.33), we get

$$\int_0^h \boldsymbol{\xi}_n \frac{d^2 Z_n}{dy^2} dy = \int_0^h Z_n \frac{d^2 \boldsymbol{\xi}_n}{dy^2} dy. \qquad (3.42)$$

Therefore, (3.40) takes the form

$$\int_0^h Z_n \frac{d^2 \boldsymbol{\xi}_n}{dy^2} dy + \gamma_n^2 \int_0^h \boldsymbol{\xi}_n Z_n dy = 0. \qquad (3.43)$$

But from (3.34), we know

$$(\boldsymbol{\xi}_n)_m = \xi_{nm} = \Lambda_m \cos(\frac{m\pi}{h}); \quad m = 0, 1, 2, ... \qquad (3.44)$$

Thus, (3.43) can be replaced as

$$\int_0^h (\frac{m\pi}{h})^2 \xi_{nm} Z_n dy + \gamma_n^2 \int_0^h \xi_{nm} Z_n dy = 0. \quad m = 0, 1, 2, ... \qquad (3.45)$$

Now from (3.37), we have

$$Z_n = \sum_{p=0}^{\infty} B_{np} \xi_{np},$$

which on using into (3.45) leads to

$$\int_0^h \sum_{p=0}^{\infty} (\frac{m\pi}{h})^2 B_{np} \xi_{np} \xi_{nm} dy + \gamma_n^2 \int_0^h \sum_{p=0}^{\infty} B_{np} \xi_{np} \xi_{nm} dy. \qquad (3.46)$$

On using the (3.36), we arrive at

$$\sum_{p=0}^{\infty} (\frac{m\pi}{h})^2 B_{np} \delta_{pm} + \gamma_n^2 \sum_{p=0}^{\infty} B_{np} \delta_{pm} = 0, \quad m = 0, 1, 2, ... \qquad (3.47)$$

In matrix form, (3.47) can be written as

$$N_1 \boldsymbol{B} + \gamma_n^2 I \boldsymbol{B} = 0, \tag{3.48}$$

where

$$N_1 = \begin{pmatrix} 0 & 0 & 0 & \dots & 0 & \dots \\ 0 & \frac{\pi^2}{h^2} & 0 & \dots & 0 & \dots \\ \vdots & \vdots & \vdots & \vdots & \vdots & \vdots \\ 0 & 0 & 0 & 0 & \frac{m^2\pi^2}{h^2} & \dots \\ \vdots & \vdots & \vdots & \vdots & \vdots & \vdots \end{pmatrix}. \tag{3.49}$$

But since $\gamma_n^2 = k^2 - s_n^2$, therefore we may write

$$s_n^2 \boldsymbol{B} = N \boldsymbol{B} \tag{3.50}$$

where

$$N = k^2 I + N_1.$$

Note that N is a known matrix whose eigenvalues are equal to $s_n^2 \; n = 0, 1, 2, \dots$ and eigenvectors are X. The resulting field potential takes the form

$$\phi(x, y) = \boldsymbol{\xi}^t X D(x) \boldsymbol{A} \tag{3.51}$$

where

$$D(x) = \begin{pmatrix} e^{is_0 x} & 0 & 0 & \dots & 0 & \dots \\ 0 & e^{is_1 x} & 0 & \dots & 0 & \dots \\ \vdots & \vdots & e^{is_2 x} & 0 & 0 & \dots \\ \vdots & \vdots & \vdots & \vdots & \vdots & \vdots \\ 0 & 0 & 0 & 0 & e^{is_n x} & \dots \\ \vdots & \vdots & \vdots & \vdots & \vdots & \vdots \end{pmatrix} \tag{3.52}$$

and

$$\boldsymbol{A}^t = \begin{bmatrix} A_0 & A_1 & \dots & A_n & \dots \end{bmatrix}. \tag{3.53}$$

On differentiating (3.51) with respect to x

$$\phi_x = \boldsymbol{\xi}^t X \frac{d}{dx} D(x) \boldsymbol{A}. \tag{3.54}$$

By matching the propagating modes with executing modes

$$\boldsymbol{\xi}^t X \frac{d}{dx} D(x) \Big|_{x=0} \boldsymbol{A} = \begin{cases} 0, & 0 \leq y < h_1 \\ U, & h_1 \leq y \leq h_2 \\ 0, & h_2 < y \leq h \end{cases}, \tag{3.55}$$

where

$$\frac{d}{dx} D(x) = \begin{pmatrix} is_0 e^{is_0 x} & 0 & 0 & \cdots & 0 & \cdots \\ 0 & is_1 e^{is_1 x} & 0 & \cdots & 0 & \cdots \\ \vdots & \vdots & is_2 e^{is_2 x} & 0 & 0 & \cdots \\ \vdots & \vdots & \vdots & \vdots & \vdots & \vdots \\ 0 & 0 & 0 & 0 & is_n e^{is_n x} & \cdots \\ \vdots & \vdots & \vdots & \vdots & \vdots & \vdots \end{pmatrix}. \tag{3.56}$$

On multiplying (3.55) with $\boldsymbol{\xi}$ and integrating from 0 to h

$$\int_0^h \boldsymbol{\xi} \boldsymbol{\xi}^t dy X \frac{d}{dx} D(x) \Big|_{x=0} \boldsymbol{A} = U \int_{h_1}^{h_2} \boldsymbol{\xi}(y) dy, \tag{3.57}$$

or

$$iX \frac{d}{dx} D(x) \Big|_{x=0} \boldsymbol{A} = U\boldsymbol{Q}, \tag{3.58}$$

where

$$\boldsymbol{Q} = \int_{h_1}^{h_2} \boldsymbol{\xi}(y) dy. \tag{3.59}$$

From (3.58), the unknown $\boldsymbol{A}$ can be evaluated as

$$\boldsymbol{A} = iD_0^{-1} X^{-1} \boldsymbol{Q} U \tag{3.60}$$

where

$$D_0 = \begin{pmatrix} s_0 & 0 & 0 & \ldots & 0 & \ldots \\ 0 & s_1 & 0 & \ldots & 0 & \ldots \\ \vdots & \vdots & s_2 & 0 & 0 & \ldots \\ \vdots & \vdots & \vdots & \vdots & \vdots & \vdots \\ 0 & 0 & 0 & 0 & s_n & \ldots \\ \vdots & \vdots & \vdots & \vdots & \vdots & \vdots \end{pmatrix}. \tag{3.61}$$

3.3 Rigid-Impedance

In this case one wall at $y = 0$ is acoustically rigid while the surface at $y = h$ is impedance. The boundary conditions for this semi-infinite duct are

$$\frac{\partial \phi}{\partial y} = 0, \quad y = 0, \quad 0 < x < \infty, \tag{3.62}$$

$$\phi + \frac{\partial \phi}{\partial y} = 0, \quad y = h, \quad 0 < x < \infty. \tag{3.63}$$

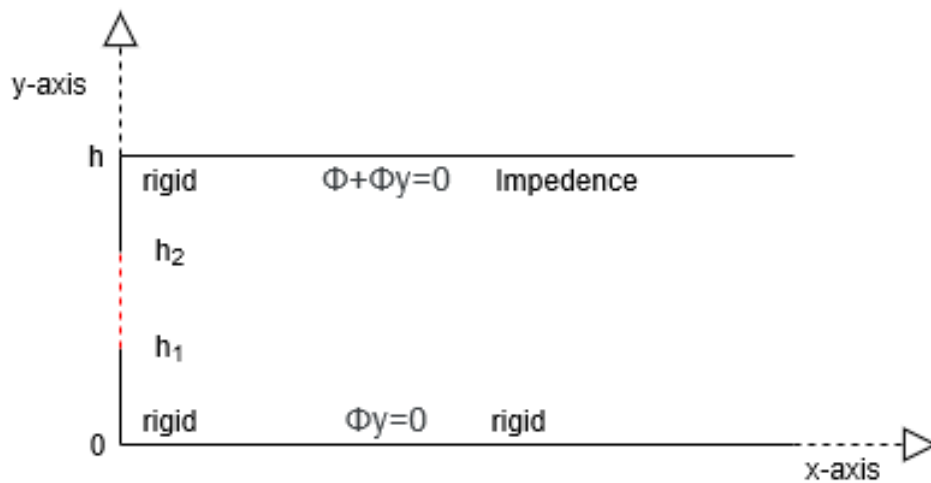Using the physical configuration of the duct having impedance and rigid boundaries is shown in Figure 3.3.

Figure 3.3: The geometry of the duct having rigid and impedance walls

Consider the duct is radiated with a plane piston lying along vertical wall $h_1 \leq y \leq h_2$ at $x = 0$, moving with constant velocity U. The velocity condition at $x = 0$

can be stated as

$$\frac{\partial \phi}{\partial x} = \begin{cases} 0, & 0 \leq y < h_1 \\ U, & h_1 \leq y \leq h_2 \\ 0, & h_2 < y \leq h \end{cases} . \tag{3.64}$$

Propagation of waveforms in duct region can be determined through Mode-matching and Multi-model techniques which are comprehensively discussed in the next subsections.

• Mode-matching Solution

The wave formulation of propagating modes can be reveals by using separation of variable method, for this we assume

$$\phi(x, y) = X(x)Y(y), \tag{3.65}$$

which on using into (3.5) leads to

$$\frac{Y''}{Y} + k^2 = -\frac{X''}{X} = \eta^2 \quad \text{(say)}. \tag{3.66}$$

On solving (3.66), we obtain

$$X(x) = c_5 e^{i\eta x} + c_6 e^{-i\eta x}, \tag{3.67}$$

and

$$Y(y) = c_7 \cos \tau y + c_8 \sin \tau y, \tag{3.68}$$

where $\tau = \sqrt{k^2 - \eta^2}$ and $c_1 - c_4$ are arbitrary constants. Boundary condition (3.62) implies that $c_8 = 0$ and to obtain non trivial form of solution from (3.63) we conclude τ are the roots of characteristics equation

$$\cos(\tau h) - \alpha \tau \sin(\tau h) = 0. \tag{3.69}$$

There are infinite many τ_n for which (3.69) holds. These roots can be found numerically by using Newton Raphson or secant method. Eigenfunctions obtained from $Y_n = \cos(\tau_n y)$, $n = 0, 1, 2, \ldots$ are orthogonal in nature and satisfy

$$\int_0^h Y_m(y)Y_n(y) = 0, \quad \text{when} \quad m \neq n, \tag{3.70}$$

and

$$\int_0^h Y_m(y)Y_n(y) = \frac{h}{2}, \quad \text{when} \quad m = n. \tag{3.71}$$

We can combine (3.70) to (3.71) to get the orthonormal relation

$$\int_0^h \psi_m(y)\psi_n(y)dy = \delta_{mn}, \tag{3.72}$$

where $\psi_m(y)$ are orthonormal function defined by

$$\psi_m = \sqrt{\frac{2}{h}}\cos(\tau_m y), \tag{3.73}$$

Therefore, the propagating wave in positive $x-$direction can be given as

$$\phi(x, y) = \sum_{n=0}^{\infty} A_n \psi_n(y)e^{i\eta_n x}, \tag{3.74}$$

where $\eta_n = \sqrt{k^2 - \tau_n^2}$, represents the nth mode wave number. A_n is the amplitude of nth mode which is unknown. To find A_n, we coincide here the executing modes with the normal velocity modes at $x = 0$. On using (3.74) into (3.64), we obtain

$$i\sum_{n=0}^{\infty} A_n \psi_n(y)\eta_n = \begin{cases} 0, & 0 \leq y < h_1 \\ U, & h_1 \leq y \leq h_2 \\ 0, & h_2 < y \leq h \end{cases}. \tag{3.75}$$

On multiplying (3.75) with $\psi_m(y)$ and integrating from 0 to h, we get

$$i\sum_{m=0}^{\infty} A_n \eta_n \int_0^h \psi_n(y)\psi_m(y)dy = U \int_{h_1}^{h_2} \psi_m(y)dy. \tag{3.76}$$

By invoking orthonormal relation (3.72), (3.76) leads to

$$\sum_{m=0}^{\infty} A_n \eta_n \delta_{mn} = iU \int_{h_1}^{h_2} \psi_m(y) dy \tag{3.77}$$

or

$$A_m = \frac{-iU}{\eta_m} Q_m, \tag{3.78}$$

where

$$Q_m = \int_{h_1}^{h_2} \psi_m(y) dy$$
$$= \sqrt{\frac{2}{h}} \left\{ \sin(\tau_m h_2) - \sin(\tau_m h_1) \right\}. \tag{3.79}$$

• Multi-modal Approach

Now to find the solution of our problem with the aid of Multi-modal approach, we assume insatz

$$\phi(x, y) = \sum_{n=0}^{\infty} A_n Z_n(y) e^{is_n x}. \tag{3.80}$$

By using (3.80) into (3.5) and on using boundary conditions (3.62)-(3.63), we respectively found

$$\frac{d^2 Z_n}{dy^2} + \gamma_n^2 Z_n = 0 \tag{3.81}$$

and

$$Z_n'(0) = 0 \tag{3.82}$$

$$Z_n(h) + \alpha Z_n{}'(h) = 0 \tag{3.83}$$

where $\gamma_n = \sqrt{k^2 - s_n^2}$, prime on involved variable shows the differentiation. We construct here an eigenvalue problem to determine the unknowns A_n, Z_n and s_n.

• Eigenvalue Problem

$$\frac{d^2 \xi_n(y)}{dy^2} + \alpha_n^2 \xi_n(y) = 0, \tag{3.84}$$

$$\xi_n'(0) = 0, \tag{3.85}$$

$$\xi_n'(h) = 0. \tag{3.86}$$

By the aid of (3.85) and (3.86), we solve (3.84) to get the orthonormal form of $\xi_n(y)$ as

$$\xi_n = \Lambda_n \cos(\alpha_n y) \tag{3.87}$$

where

$$\alpha_n = \frac{n\pi}{h}, \tag{3.88}$$

and

$$\int_0^h \xi_n(y)\xi_m(y) = \delta_{mn}. \tag{3.89}$$

Let we assume $Z_n(y)$ as the linear combination of ξ_m as

$$Z_n(y) = \sum_{m=0}^{\infty} B_{nm}\xi_{nm}(y) = \boldsymbol{\xi}_n^t \boldsymbol{B}_n \tag{3.90}$$

where

$$\boldsymbol{\xi}_n^t = \begin{bmatrix} \xi_{n0} & \xi_{n1} & \cdots & \xi_{nm} & \cdots \end{bmatrix}, \tag{3.91}$$

and

$$\boldsymbol{B}_n^t = \begin{bmatrix} B_{n0} & B_{n1} & \cdots & B_{nm} & \cdots \end{bmatrix}. \tag{3.92}$$

Note that t on super script of $\boldsymbol{\xi}_n$ and $\boldsymbol{B}_n$ represents the transpose of a vector. On multiplying (3.81) with $\boldsymbol{\xi}_n$ and integrating over y from 0 to h, we get

$$\int_0^h \boldsymbol{\xi}_n \frac{d^2 Z_n}{dy^2} dy + \gamma_n^2 \int_0^h \boldsymbol{\xi}_n Z_n dy = 0. \tag{3.93}$$

The solution of second integral of (3.93) can be obtained by performing integration by parts as

$$\int_0^h \boldsymbol{\xi}_n \frac{d^2 Z_n}{dy^2} dy = \left(\boldsymbol{\xi}_n(y)\frac{dZ_n}{dy}\right)\Big|_0^h - \left(\frac{d\boldsymbol{\xi}_n}{dy}Z_n\right)\Big|_0^h + \int_0^h Z_n \frac{d^2\boldsymbol{\xi}_n}{dy^2} dy. \tag{3.94}$$

On using boundary conditions (3.82)-(3.83) and (3.85)-(3.86), we get

$$\int_0^h \boldsymbol{\xi}_n \frac{d^2 Z_n}{dy^2} dy = -\frac{1}{\alpha} \boldsymbol{\xi}_n(h) Z_n(h) + \int_0^h Z_n \frac{d^2 \boldsymbol{\xi}_n}{dy^2} dy. \qquad (3.95)$$

Therefore, (3.93) takes the form

$$-\frac{1}{\alpha} \boldsymbol{\xi}_n(h) Z_n(h) + \int_0^h Z_n \frac{d^2 \boldsymbol{\xi}_n}{dy^2} dy + \gamma_n^2 \int_0^h \boldsymbol{\xi}_n Z_n dy = 0. \qquad (3.96)$$

From (3.87), we can write

$$(\boldsymbol{\xi}_n)_m = \xi_{nm} = \Lambda_m \cos(\frac{m\pi}{h}); \quad m = 0, 1, 2, ... \qquad (3.97)$$

On using (3.97) into (3.96), we obtain

$$-\frac{1}{\alpha} \boldsymbol{\xi}_n(h) Z_n(h) - \int_0^h (\frac{m\pi}{h})^2 \boldsymbol{\xi}_n Z_n dy + \gamma_n^2 \int_0^h \boldsymbol{\xi}_n Z_n dy = 0, \qquad (3.98)$$

or

$$-\frac{1}{\alpha} \xi_{nm}(h) Z_n(h) - \int_0^h (\frac{m\pi}{h})^2 \xi_{nm} Z_n dy + \gamma_n^2 \int_0^h \xi_{nm} Z_n dy = 0. \qquad (3.99)$$

As

$$Z_n = \sum_{p=0}^\infty B_{np} \xi_{np}$$

therefore, (3.99) can be formulated as

$$-\frac{1}{\alpha} \sum_{p=0}^\infty B_{np} \xi_{np} \xi_{nm} - \int_0^h \sum_{p=0}^\infty (\frac{m\pi}{h})^2 B_{np} \xi_{np} \xi_{nm} dy + \gamma_n^2 \int_0^h \sum_{p=0}^\infty B_{np} \xi_{np} \xi_{nm} dy \quad (3.100)$$

or

$$-\frac{1}{\alpha} \sum_{p=0}^\infty B_{np}(h) \xi_{np}(h) \xi_{nm}(h) - \sum_{p=0}^\infty (\frac{m\pi}{h})^2 B_{np} \delta_{pm} + \gamma_n^2 \sum_{p=0}^\infty B_{np} \delta_{pm} = 0. \quad (3.101)$$

Equation (3.101) in a matrix form can be written as

$$-\frac{1}{\alpha} N_1 \boldsymbol{B} - N_2 I \boldsymbol{B} + \gamma_n^2 I \boldsymbol{B} = 0, \qquad (3.102)$$

where

$$
N_1 = \begin{pmatrix}
\xi_{0n}(h)\xi_{0n}(h) & \xi_{0n}(h)\xi_{1n}(h) & \xi_{0n}(h)\xi_{2n}(h) & \cdots & \xi_{0n}(h)\xi_{mn}(h) & \cdots \\
\xi_{1n}(h)\xi_{0n}(h) & \xi_{1n}(h)\xi_{1n}(h) & \xi_{1n}(h)\xi_{2n}(h) & \cdots & \xi_{1n}(h)\xi_{mn}(h) & \cdots \\
\xi_{2n}(h)\xi_{0n}(h) & \xi_{2n}(h)\xi_{1n}(h) & \xi_{2n}(h)\xi_{2n}(h) & \cdots & \xi_{2n}(h)\xi_{mn}(h) & \cdots \\
\vdots & \vdots & \vdots & \vdots & \vdots & \vdots \\
\xi_{pn}(h)\xi_{0n}(h) & \xi_{pn}(h)\xi_{1n}(h) & \xi_{pn}(h)\xi_{2n}(h) & \cdots & \xi_{pn}(h)\xi_{mn}(h) & \cdots \\
\vdots & \vdots & \vdots & \vdots & \vdots & \vdots
\end{pmatrix}
\tag{3.103}
$$

and

$$
N_2 = \begin{pmatrix}
0 & 0 & 0 & \cdots & 0 \\
0 & \frac{\pi^2}{h^2} & \vdots & \vdots & \vdots \\
\vdots & \vdots & \vdots & \vdots & \vdots \\
0 & 0 & 0 & \frac{m^2\pi^2}{h^2} & \vdots \\
\vdots & \vdots & \vdots & \vdots & \vdots
\end{pmatrix}.
\tag{3.104}
$$

As $\gamma_n^2 = k^2 - s_n^2$, therefore (3.102) can be written as

$$
s_n^2 \boldsymbol{B} = N\boldsymbol{B}
\tag{3.105}
$$

where

$$
N = Ik^2 - \frac{1}{\alpha}N_1 - N_2 I.
\tag{3.106}
$$

Note that the matrix N contain the eigenvalues s_n^2; $n = 0, 1, 2, ...$ and eigenvectors X. Being aware of eigenvalues and eigenvectors the resulting field potential in semi infinite duct can be written as

$$
\phi(x, y) = \boldsymbol{\xi}^t X D(x) \boldsymbol{A}
\tag{3.107}
$$

where

$$D(x) = \begin{pmatrix} e^{is_0 x} & 0 & 0 & \ldots & 0 & \ldots \\ 0 & e^{is_1 x} & 0 & \ldots & 0 & \ldots \\ \vdots & \vdots & e^{is_2 x} & 0 & 0 & \ldots \\ \vdots & \vdots & \vdots & \vdots & \vdots & \vdots \\ 0 & 0 & 0 & 0 & e^{is_n x} & \ldots \\ \vdots & \vdots & \vdots & \vdots & \vdots & \vdots \end{pmatrix} \tag{3.108}$$

and

$$\boldsymbol{A}^t = \begin{bmatrix} A_0 & A_1 & \ldots & A_n & \ldots \end{bmatrix}. \tag{3.109}$$

On differentiating (3.107) with respect to x

$$\phi_x = \boldsymbol{\xi}^t X \frac{d}{dx} D(x) \boldsymbol{A} \tag{3.110}$$

By comparing the propagating and executing modes

$$\boldsymbol{\xi}^t X \frac{d}{dx} D(x) \Bigg|_{x=0} \boldsymbol{A} = \begin{cases} 0, & 0 \le y < h_1 \\ U, & h_1 \le y \le h_2 \\ 0, & h_2 < y \le h \end{cases}, \tag{3.111}$$

where

$$\frac{d}{dx} D(x) = \begin{pmatrix} is_0 e^{is_0 x} & 0 & 0 & \ldots & 0 & \ldots \\ 0 & is_1 e^{is_1 x} & 0 & \ldots & 0 & \ldots \\ \vdots & \vdots & is_2 e^{is_2 x} & 0 & 0 & \ldots \\ \vdots & \vdots & \vdots & \vdots & \vdots & \vdots \\ 0 & 0 & 0 & 0 & is_n e^{is_n x} & \ldots \\ \vdots & \vdots & \vdots & \vdots & \vdots & \vdots \end{pmatrix}. \tag{3.112}$$

On multiplying (3.111) with $\boldsymbol{\xi}$ and integrating from 0 to h

$$\int_0^h \boldsymbol{\xi}\boldsymbol{\xi}^t dy X \frac{d}{dx} D(x)\bigg|_{x=0} \boldsymbol{A} = U \int_{h_1}^{h_2} \boldsymbol{\xi}(y)dy, \tag{3.113}$$

or

$$iX\frac{d}{dx}D(x)\bigg|_{x=0} \boldsymbol{A} = U\boldsymbol{Q}, \tag{3.114}$$

where

$$\boldsymbol{Q} = \int_{h_1}^{h_2} \boldsymbol{\xi}(y)dy. \tag{3.115}$$

From (3.114), the unknown $\boldsymbol{A}$ can be evaluated as

$$\boldsymbol{A} = iD_0^{-1}X^{-1}\boldsymbol{Q}U \tag{3.116}$$

where

$$D_0 = \begin{pmatrix} s_0 & 0 & 0 & \cdots & 0 & \cdots \\ 0 & s_1 & 0 & \cdots & 0 & \cdots \\ \vdots & \vdots & s_2 & 0 & 0 & \cdots \\ \vdots & \vdots & \vdots & \vdots & \vdots & \vdots \\ 0 & 0 & 0 & 0 & s_n & \cdots \\ \vdots & \vdots & \vdots & \vdots & \vdots & \vdots \end{pmatrix}. \tag{3.117}$$

3.4   Numerical Results

Here the numerical results are shown. As the modelled problems having excitation from the plane piston are solved by using Mode-matching technique and Multi-modal technique. For numerical computation the dimensional heights h, h_1 and h_2 are taken to be 0.2m, 0.05m and 0.1m, respectively. The speed of sound $c = 343.5$m/s and $k = 2\pi f/c$, where f is frequency measured in Hertz. The velocity U of the piston is taken 10m/s, 80m/s and 180m/s and the absolute value of fundamental mode $|A_0|$ and the absolute secondary mode $|A_1|$ are plotted against frequency f. From Figs. 3.4 and 3.5 it can be seen that by changing the velocity of the piston and magnitude of amplitudes of propagating waves are changed. Moreover, a good agreement between Mode-matching results (shown with solid

lines in Figs 3.4 and 3.5) and Multi-modal results (shown with dashed lines) is found.
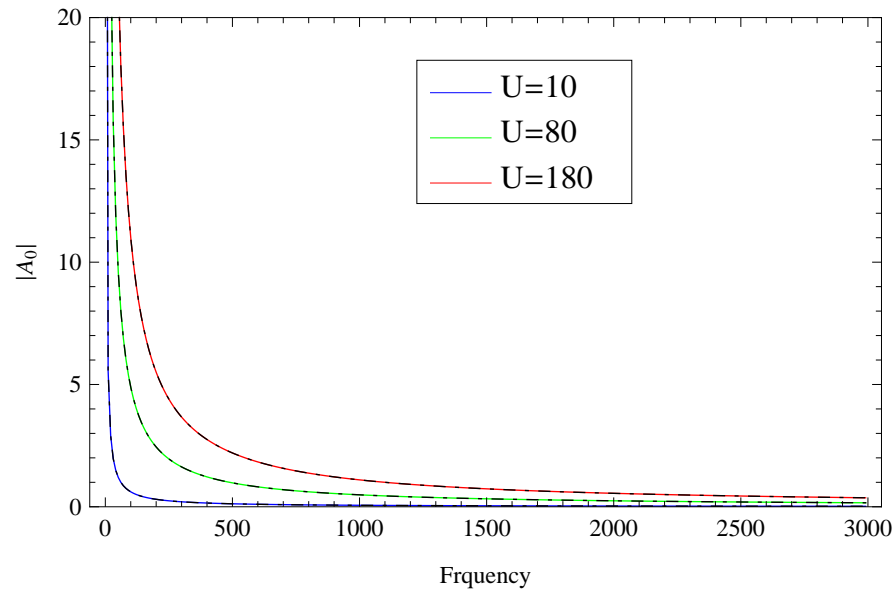

Figure 3.4: The absolute value of fundamental mode $|A_0|$ against frequency.
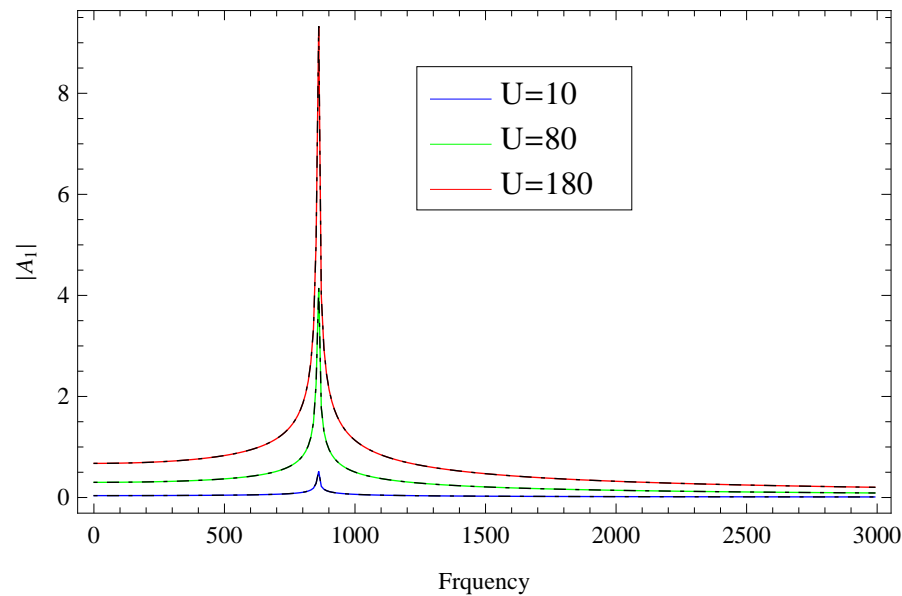

Figure 3.5: The absolute value of secondary mode $|A_1|$ against frequency.

Similarly the graphs plotted against frequency and amplitudes of the problem discussed section 3.3. are shown in Figs. 3.6 and 3.7. The numericals results are obtained by using Mode-matching and Multi-modal techniques. For the solution the heights of vertical wall of geometry are respectively taken as $h = 0.2$m, $h_1 =$

0.05m, $h_2 = 0.1$m and $k = 2\pi f/c$, where $c = 343.5$m/s, and f is the frequency and is measured in Hertz.
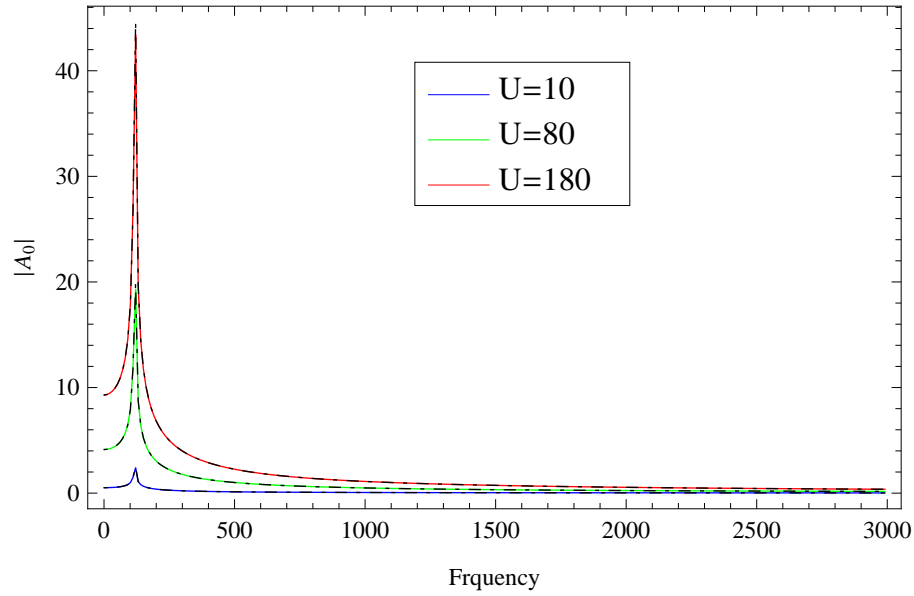
Figure 3.6: The absolute value of fundamental mode $|A_0|$ against frequency.
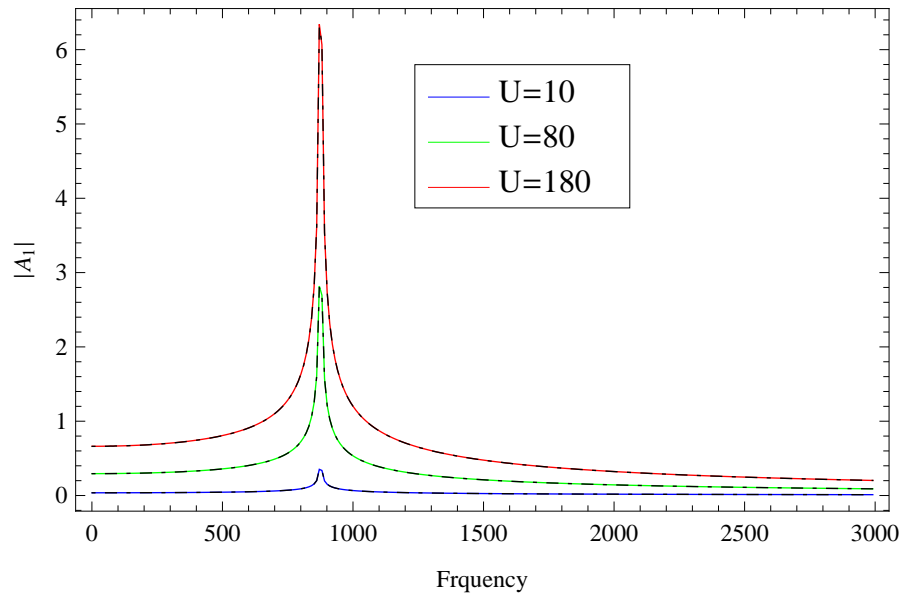
Figure 3.7: The absolute value of secondary mode $|A_1|$ against frequency.

The graphs are plotted against frequency f and amplitudes $|A_0|$ and $|A_1|$. These modes are produced by plane piston of velocity U taken as 10m/s, 80m/s and 180m/s. It can be clearly seen from Figs. 3.6 and 3.7 that absolute values of $|A_0|$ and $|A_1|$ are increasing by increasing the velocity of the plane piston. The results

obtained from Mode-matching (shown with solid lines) and Multi-modal (shown with dashed lines) are supported well.

Chapter 4

Acoustic Propagation and Scattering through the Lined Cavities

In this chapter, we consider here a waveguide having absorbing lining in central region. The geometry of propagating waves in lined duct having impedance and rigid boundaries is shown in figure 4.1. The mathematical formulation of the problem is described in section 4.1. The propagation of waves in double cavity of honey comb layers is discussed in 4.1.1. The impedance boundary conditions are formulated with the aid of field potential and by using velocity conditions. The Multi-modal method is used to solve the governing BVP. In section 4.2 the propagation and scattering of travelling waveforms in inlet and outlet regions are described. The propagating modes in central region is discussed in 4.2.2. The eigenmodes of central region containing liner cavities are determined by Multi-modal approach. The field potential in duct regions is written as sum of transverse modes then reflection and transmission coefficients are obtained by using pressure and velocity conditions at interfaces. The numerical results are provided at the end of the Chapter.

4.1   Mathematical Formulation

Consider an acoustic plane wave propagating form negative x-direction towards $x = 0$, in an infinite waveguide. At $x = 0$, it will spread into different directions of infinite reflected and transmitted modes. The waveguide is divided into three regions. First inlet; having incident and reflected fields and third outlet; which contains outgoing field, whereas the second region is lined through locally reacting liners where in attenuation take place. The inside of the waveguide is filled with compressible fluid of density ρ and sound speed c. The physical configuration of the waveguide is as shown in Figure 4.1.
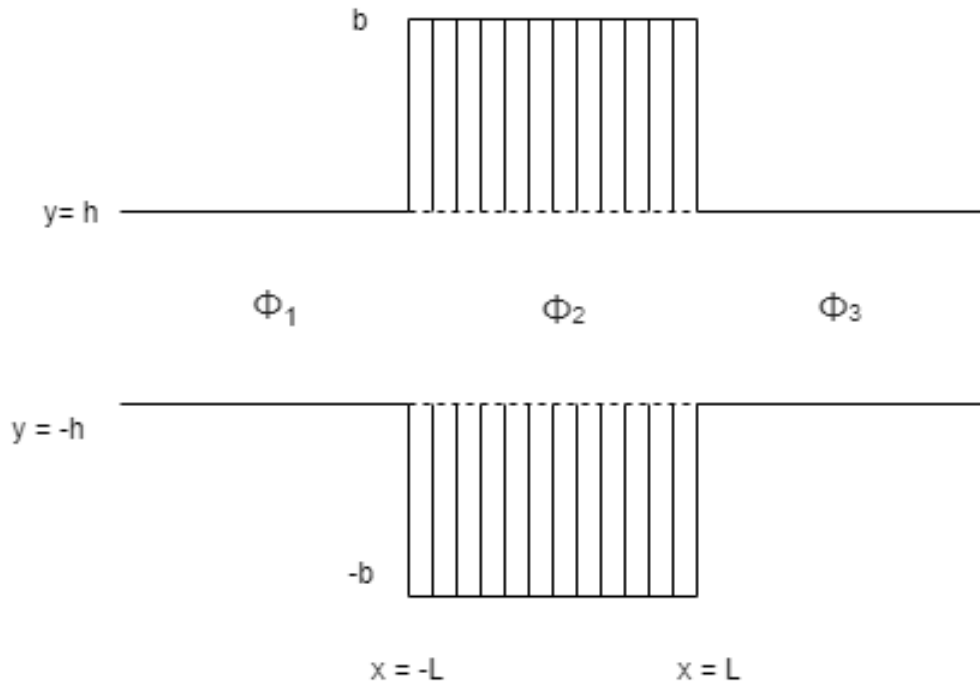

Figure 4.1: The geometrical configuration of the waveguide.

The acoustic pressure p and velocity vector $\mathbf{v}$ in the waveguide regions are

$$p = -\rho \frac{\partial \Phi}{\partial t} \tag{4.1}$$

and

$$\mathbf{v} = \nabla \Phi \tag{4.2}$$

respectively. Here $\Phi(x, y, t)$ represents the field potential in the waveguide and satisfies the wave equation

$$\frac{\partial^2 \Phi}{\partial x^2} + \frac{\partial^2 \Phi}{\partial y^2} = \frac{1}{c^2} \frac{\partial^2 \Phi}{\partial t^2}. \tag{4.3}$$

Assuming the harmonic time dependence $e^{-i\omega t}$ having radial frequency ω, we may write

$$\Phi(x, y, t) = \phi(x, y) e^{-i\omega t}, \tag{4.4}$$

where $\phi(x, y)$ stands for the time independent field potential in the waveguide. By using (4.4) into (4.3), we get Helmholtz's equation

$$\frac{\partial^2 \phi}{\partial x^2} + \frac{\partial^2 \phi}{\partial y^2} + k^2 \phi = 0, \tag{4.5}$$

where $k = \omega/c$ be the wave number. For convenience we divide the field potential $\phi(x, y)$ are

$$\phi(x, y) = \begin{cases} \phi_1(x, y), & -\infty < x < -L, & -h < y < h, \\ \phi_2(x, y), & -L < x < L, & -h < y < h, \\ \phi_3(x, y), & L < x < \infty, & -h < y < h \end{cases} \tag{4.6}$$

As the boundaries of the waveguide of first and third regions are acoustically rigid i.e.

$$\frac{\partial \phi_1}{\partial y} = 0, \qquad y = \pm h, \qquad -\infty < x < 0, \tag{4.7}$$

$$\frac{\partial \phi_3}{\partial y} = 0, \qquad y = \pm h, \qquad L < x < \infty. \tag{4.8}$$

4.1.1   Conditions for Liner

Now to derive the condition associated with the reacting liners used in the second region of waveguide, the impedance formulation is [1]

$$\mathfrak{Z}(y) = \frac{p}{\mathbf{v}.\mathbf{n}}, \tag{4.9}$$

where **n** is inward directed normal vector. Therefore in terms of fluid velocity potential ϕ, the impedance condition takes the form

$$\mathfrak{Z}(y) = \frac{i\rho\omega\phi}{\nabla\phi.\mathbf{n}}, \tag{4.10}$$

or

$$\mathfrak{Z}(y) = \frac{i\rho\omega\phi}{\frac{\partial\phi}{\partial y}}. \tag{4.11}$$

To determine the impedance condition at $y = \pm h$, we consider a single honeycomb layer of reacting liners as shown in Figure 4.2.
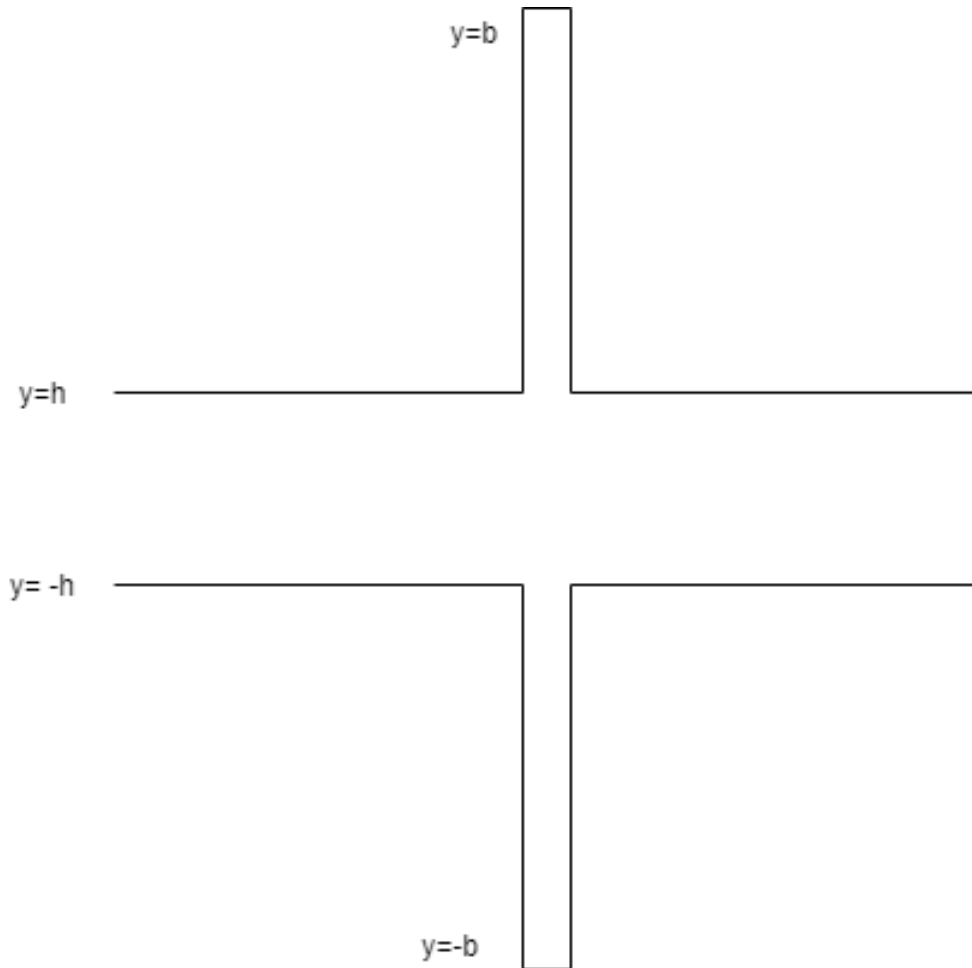

Figure 4.2: The geometry of single honeycomb layer

In the single reactive honeycomb layer backed by rigid wall, the field potential in one dimensional form satisfies the wave equation

$$\frac{d^2\varphi}{dy^2} + k^2\varphi(y) = 0. \quad -b \leq y \leq -h \quad \text{and} \quad h \leq y \leq b \tag{4.12}$$

On solving (4.12), we found

$$\varphi(y) = c_1 \cos(ky) + c_2 \sin(ky), \tag{4.13}$$

which respectively corresponds the pressure p and velocity v as

$$\text{p} = \rho i\omega \left\{ c_1 \cos(ky) + c_2 \sin(ky) \right\} \tag{4.14}$$

and

$$\text{v} = k \left\{ -c_1 \sin(ky) + c_2 \cos(ky) \right\}. \tag{4.15}$$

Therefore, the impedance of the liner

$$\Im(y) = \frac{i\omega\rho \left\{ c_1 \cos(ky) + c_2 \sin(ky) \right\}}{k \left\{ -c_1 \sin(ky) + c_2 \cos(ky \right\}} \tag{4.16}$$

or

$$\Im(y) = \frac{i\omega\rho \left\{ \frac{c_1}{c_2} \cos(ky) + \sin(ky) \right\}}{k \left\{ -\frac{c_1}{c_2} \sin(ky) + \cos(ky \right\}}. \tag{4.17}$$

Since the reactive liner is backed by rigid wall at $y = \pm b$, therefore

$$\left\{ -c_1 \sin(kb) + c_2 \cos(kb) \right\} = 0 \tag{4.18}$$

and

$$\left\{ -c_1 \sin(-kb) + c_2 \cos(-kb) \right\} = 0. \tag{4.19}$$

From (4.18)

$$\frac{c_1}{c_2} = \frac{\cos(kb)}{\sin(kb)} \tag{4.20}$$

and from (4.19), we get

$$\frac{c_1}{c_2} = -\frac{\cos(kb)}{\sin(kb)}. \tag{4.21}$$

By using (4.20) and (4.21) into (4.17), we find

$$\mathfrak{Z}(y) = -\frac{i\omega\rho}{k}\frac{\cos[k(y-b)]}{\sin[k(y-b)]}, \quad \text{for} \quad h \leq y \leq b, \tag{4.22}$$

and

$$\mathfrak{Z}(y) = -\frac{i\omega\rho}{k}\frac{\cos[k(y+b)]}{\sin[k(y+b)]} \quad \text{for} \quad -b \leq y \leq -h. \tag{4.23}$$

Thus, for $y = \pm h$, from (4.22) and (4.23), we get

$$\mathfrak{Z}(\pm h) = \pm\frac{i\omega\rho}{k\tan[k(b-h)]}. \tag{4.24}$$

Now from (4.11), we may write

$$\frac{\partial\phi}{\partial y} - \frac{i\omega\rho}{\mathfrak{Z}(y)}\phi = 0, \tag{4.25}$$

which at $y = -h$

$$\frac{\partial\phi}{\partial y} + \xi(k)\phi = 0, \quad 0 \leq x \leq L \tag{4.26}$$

and at $y = +h$

$$\frac{\partial\phi}{\partial y} - \xi(k)\phi = 0, \quad 0 \leq x \leq L \tag{4.27}$$

where

$$\xi(k) = k\tan[k(b-h)]$$

is known the normalize impedance.

4.2 Travelling Waveforms in Waveguide

Here we determine the formulation of propagating modes in inlet/outlet and central region.

4.2.1 Propagating Modes in inlet/outlet

The formulation of propagating modes in the inlet/outlet subjected to rigid boundaries can be determined by using the separation of variable technique. For this we let

$$\phi(x, y) = X(x)Y(y), \tag{4.28}$$

which on using into (4.5) leads to

$$\frac{Y''}{Y} + k^2 = -\frac{X''}{X} = \eta^2 \quad \text{(say)}. \tag{4.29}$$

By solving (4.29), we obtain

$$X(x) = c_3 e^{i\eta x} + c_4 e^{-i\eta x} \tag{4.30}$$

and

$$Y(y) = c_5 \cos \tau y + c_6 \sin \tau y, \tag{4.31}$$

where $\tau = \sqrt{k^2 - \eta^2}$ and $c_3 - c_6$ are arbitrary constants. As we have assumed rigid boundary conditions (4.7) and (4.8) which result eigenvalues $\tau_n = (n\pi/2h)$, $n = 0, 1, 2, ...$ and the corresponding eigenfunction $Y_n(y) = \cos(\tau_n y)$, $n = 0, 1, 2, ...$ These eigenfunctions are orthogonal in nature and satisfy the orthogonality relation. For $n \geq 1$, $m \geq 1$

$$\int_{-h}^{h} Y_n(y) Y_m(y) dy = h\delta_{mn}, \tag{4.32}$$

whereas, for $m = n = 0$

$$\int_{-h}^{h} Y_0(y) Y_0(y) dy = 2h. \tag{4.33}$$

Therefore for all n, we may write the orthonormal form as

$$\psi_n = \Lambda_n \cos(\tau_n y) \tag{4.34}$$

where

$$\Lambda_n = \begin{cases} \frac{1}{\sqrt{2h}}, & n = 0, \\ \sqrt{\frac{1}{h}}, & n \geq 1 \end{cases} .$$ (4.35)

The orthonormal relation is

$$\int_{-h}^{h} \psi_m(y)\psi_n(y) = \delta_{mn}$$ (4.36)

where

$$\delta_{mn} = \begin{cases} 1 & m = n \\ 0 & m \neq 0 \end{cases} .$$

Now, the propagation of waves in first and third regions having rigid boundary conditions can be defined as

$$\phi_1(x, y) = \sum_{n=0}^{\infty} A_{1n}\psi_n(y)e^{i\eta_n x} + \sum_{n=0}^{\infty} B_{1n}\psi_n(y)e^{-i\eta_n x},$$ (4.37)

$$\phi_3(x, y) = \sum_{n=0}^{\infty} A_{3n}\psi_n(y)e^{i\eta_n(x-L)} + \sum_{n=0}^{\infty} B_{3n}\psi_n(y)e^{-i\eta_n(x-L)},$$ (4.38)

where $\{A_{1n}, B_{1n}\}$ and $\{A_{3n}, B_{3n}\}$ are the amplitudes of nth propagating modes in first and third regions and are unknowns. Note that the positive sign in exponent indicates the propagation of waves in positive x-direction and negative sign indicates the waves propagating in negative x-direction. Above equations (4.37) and (4.38) in matrix form can be written as

$$\boldsymbol{\phi}_1 = \boldsymbol{\psi}^t D_1(x)\boldsymbol{A}_1 + \boldsymbol{\psi}^t D_1(-x)\boldsymbol{B}_1,$$ (4.39)

$$\boldsymbol{\phi}_3 = \boldsymbol{\psi}^t D_1(x - L)\boldsymbol{A}_3 + \boldsymbol{\psi}^t D_1(L - x)\boldsymbol{B}_3.$$ (4.40)

where t on superscript denotes transpose of matrix.

Here $D_1(x)$ is the diagonal matrix containing the elements $e^{i\eta_n x}$ as follows

$$
D_1(x) = \begin{pmatrix}
e^{i\eta_0 x} & 0 & 0 & \dots & 0 & \dots \\
0 & e^{i\eta_1 x} & 0 & \dots & 0 & \dots \\
\vdots & \vdots & e^{i\eta_2 x} & 0 & 0 & \dots \\
\vdots & \vdots & \vdots & \vdots & \vdots & \vdots \\
0 & 0 & 0 & 0 & e^{i\eta_n x} & \dots \\
\vdots & \vdots & \vdots & \vdots & \vdots & \vdots
\end{pmatrix}, \tag{4.41}
$$

and $\boldsymbol{A}$, $\boldsymbol{B}$ are vectors such as

$$
\boldsymbol{A}^t = \begin{bmatrix} A_0 & A_1 & \dots & A_n & \dots \end{bmatrix}, \tag{4.42}
$$

$$
\boldsymbol{B}^t = \begin{bmatrix} B_0 & B_1 & \dots & B_n & \dots \end{bmatrix}. \tag{4.43}
$$

On differentiating (4.39) and (4.40) with respect to x, we will obtain

$$
\frac{\partial \phi_1}{\partial x} = \boldsymbol{\psi}^t \frac{d}{dx} D_1(x) \boldsymbol{A}_1 + \boldsymbol{\psi}^t \frac{d}{dx} D_1(-x) \boldsymbol{B}_1 \tag{4.44}
$$

and

$$
\frac{\partial \phi_3}{\partial x} = \boldsymbol{\psi}^t \frac{d}{dx} D_1(x - L) \boldsymbol{A}_3 + \boldsymbol{\psi}^t \frac{d}{dx} D_1(L - x) \boldsymbol{B}_3. \tag{4.45}
$$

4.2.2 Propagating Modes in Central Region

The central region involves reactive liners occupying the regions $-b \leq y < -h$ and $h < y < b$ whereas, the region at $-h \leq y \leq h$ is liner free region in which attenuation take place. To determine the eigenmodes of central region and to analyze the acoustic scattering in expansion chamber having two liner cavities, we use Multi-modal formulation.

Multi-modal Method

To determine the eigenmodes subject to liner conditions at $y = \pm h$, we assume insatz

$$\phi_2(x, y) = \sum_{n=0}^{\infty} A_{2n} Z_n(y) e^{is_n x}. \tag{4.46}$$

By using (4.46) into (4.5) and from (4.26)-(4.27), we obtain

$$\frac{d^2 Z_n}{dy^2} + \gamma_n^2 Z_n(y) = 0, \tag{4.47}$$

subject to boundary conditions

$$\frac{dZ_n}{dy} + \xi(k) Z_n = 0, \quad \text{at} \quad y = -h, \tag{4.48}$$

$$\frac{dZ_n}{dy} - \xi(k) Z_n = 0, \quad \text{at} \quad y = +h, \tag{4.49}$$

where

$$\gamma_n = \sqrt{k^2 - s_n^2}.$$

Note that γ_n and Z_n are unknowns. To determine these we define the related eigenvalue problem as follow.

$$\frac{d^2}{dy^2} \psi_n(y) + \alpha_n^2 \psi_n(y) = 0 \tag{4.50}$$

$$\frac{d}{dy} \psi(y) = 0 \quad y = -h \tag{4.51}$$

$$\frac{d}{dy} \psi(y) = 0 \quad y = h. \tag{4.52}$$

By solving (4.50) with the aid of (4.51) and (4.52), we get the orthonormal form of $\psi_n(y)$ as

$$\psi_n = \Lambda_n \cos[\alpha_n(y - h)] \tag{4.53}$$

which satisfies orthonormal relation

$$\int_{-h}^{h} \psi_n(y)\psi_m(y)dy = \delta_{mn} \tag{4.54}$$

where

$$\alpha_n = \frac{n\pi}{2h}; \quad n = 0, 1, 2, \dots$$

Let we denote $Z_n(y)$ as liner combination of ψ_m as

$$Z_n(y) = \sum_{m=0}^{\infty} A_{mn}\psi_{mn}(y) = \boldsymbol{\psi}_n^t \boldsymbol{A}_n \tag{4.55}$$

where $\boldsymbol{\psi}_n$ and $\boldsymbol{A}_n$ are column vectors defined by

$$\boldsymbol{\psi}_n = \begin{pmatrix} \psi_{on} \\ \psi_{1n} \\ \vdots \\ \psi_{mn} \\ \vdots \end{pmatrix} \quad \text{and} \quad \boldsymbol{A}_n = \begin{pmatrix} A_{0n} \\ A_{1n} \\ \vdots \\ A_{mn} \\ \vdots \end{pmatrix}. \tag{4.56}$$

Note that $A_{mn}; m = 0, 1, 2, \dots$ are unknowns; On multiplying $\boldsymbol{\psi}_n$ with both sides of equation (4.47), and integrate over y, we obtain also

$$\int_{-h}^{h} \boldsymbol{\psi}_n \frac{d^2 Z_n}{dy^2}dy + \gamma_n^2 \int_{-h}^{h} \boldsymbol{\psi}_n Z_n dy = 0. \tag{4.57}$$

By performing the integration by parts, the first term on the left hand side of (4.57) can be written as

$$\int_{-h}^{h} \boldsymbol{\psi}_n \frac{d^2 Z_n}{dy^2}dy = \left(\boldsymbol{\psi}_n(y)\frac{dZ_n}{dy}\right)\Big|_{-h}^{h} - \left(\frac{d\boldsymbol{\psi}_n}{dy}Z_n\right)\Big|_{-h}^{h} + \int_{-h}^{h} Z_n \frac{d^2\boldsymbol{\psi}_n}{dy^2}dy. \tag{4.58}$$

By substituting the boundary conditions (4.48)-(4.49) and (4.51)-(4.52), we get

$$\int_{-h}^{h} \boldsymbol{\psi}_n \frac{d^2 Z_n}{dy^2}dy = \xi\boldsymbol{\psi}_n(h)Z_n(h) + \xi\boldsymbol{\psi}_n(-h)Z_n(-h) + \int_{-h}^{h} Z_n \frac{d^2\boldsymbol{\psi}_n}{dy^2}dy. \tag{4.59}$$

By putting (4.59) into (4.57), we find

$$\xi\boldsymbol{\psi}_n(h)Z_n(h) + \xi\boldsymbol{\psi}_n(-h)Z_n(-h) + \int_{-h}^{h} Z_n \frac{d^2\boldsymbol{\psi}_n}{dy^2} dy + \gamma_n^2 \int_{-h}^{h} \boldsymbol{\psi}_n Z_n dy = 0. \quad (4.60)$$

But we know that

$$\boldsymbol{\psi}_n(y) = \psi_{nm}(y) = \Lambda_m \cos(\frac{m\pi}{2h}y), \quad m = 0,1,2,... \quad (4.61)$$

Therefore (4.60) can be written as

$$\xi\boldsymbol{\psi}_n(h)Z_n(h) + \xi\boldsymbol{\psi}_n(-h)Z_n(-h) - \int_{-h}^{h} (\frac{m\pi}{2h})^2 \boldsymbol{\psi}_n Z_n dy + \gamma_n^2 \int_{-h}^{h} \boldsymbol{\psi}_n Z_n dy = 0, \quad (4.62)$$

or

$$\xi\psi_{nm}Z_n(h) + \xi\psi_{nm}Z_n(-h) - \int_{-h}^{h} (\frac{m\pi}{2h})^2 \psi_{nm}Z_n dy + \gamma_n^2 \int_{-h}^{h} \psi_{nm}Z_n dy = 0. \quad (4.63)$$

Also, we have $Z_n = \sum_{p=0}^{\infty} A_{np}\psi_{np}$, which on using into (4.63), leads to

$$\begin{aligned}
&\xi\sum_{p=0}^{\infty} A_{np}(h)\psi_{np}(h)\psi_{nm}(h) + \xi\sum_{p=0}^{\infty} A_{np}(-h)\psi_{np}(-h)\psi_{nm}(-h) \\
&- \int_{-h}^{h} \sum_{p=0}^{\infty} (\frac{m\pi}{2h})^2 A_{np}\psi_{np}\psi_{nm} dy + \gamma_n^2 \int_{-h}^{h} \sum_{p=0}^{\infty} A_{np}\psi_{np}\psi_{nm} dy = 0,
\end{aligned} \quad (4.64)$$

or

$$\begin{aligned}
&\xi\sum_{p=0}^{\infty} A_{np}(h)\xi_{np}(h)\psi_{nm}(h) + \xi\sum_{p=0}^{\infty} A_{np}(-h)\psi_{np}(-h)\psi_{nm}(-h) \\
&- \sum_{p=0}^{\infty} (\frac{m\pi}{2h})^2 A_{np}\delta_{pm} + \gamma_n^2 \sum_{p=0}^{\infty} A_{np}\delta_{pm} = 0.
\end{aligned} \quad (4.65)$$

Note that

$$\sum_{p=0}^{\infty} A_{np}(h)\psi_{np}(h)\psi_{nm}(h) = N_1 \boldsymbol{A} \quad (4.66)$$

and

$$\sum_{p=0}^{\infty} A_{np}(-h)\psi_{np}(-h)\psi_{nm}(h) = N_2 \boldsymbol{A} \tag{4.67}$$

where

$$N_1 = \begin{pmatrix} \psi_{0n}(h)\psi_{0n}(h) & \psi_{0n}(h)\psi_{1n}(h) & \psi_{0n}(h)\psi_{2n}(h) & \dots & \psi_{0n}(h)\psi_{mn}(h) & \dots \\ \psi_{1n}(h)\psi_{0n}(h) & \psi_{1n}(h)\psi_{1n}(h) & \psi_{1n}(h)\psi_{2n}(h) & \dots & \psi_{1n}(h)\psi_{mn}(h) & \dots \\ \psi_{2n}(h)\psi_{0n}(h) & \psi_{2n}(h)\psi_{1n}(h) & \psi_{2n}(h)\psi_{2n}(h) & \dots & \psi_{2n}(h)\psi_{mn}(h) & \dots \\ \vdots & \vdots & \vdots & \vdots & \vdots & \vdots \\ \psi_{pn}(h)\psi_{0n}(h) & \psi_{pn}(h)\psi_{1n}(h) & \psi_{pn}(h)\psi_{2n}(h) & \dots & \psi_{pn}(h)\psi_{mn}(h) & \dots \\ \vdots & \vdots & \vdots & \vdots & \vdots & \vdots \end{pmatrix} \tag{4.68}$$

$$N_2 = \begin{pmatrix} \psi_{0n}(-h)\psi_{0n}(-h) & \psi_{0n}(-h)\psi_{1n}(-h) & \dots & \psi_{0n}(-h)\psi_{mn}(-h) & \dots \\ \psi_{1n}(-h)\psi_{0n}(-h) & \psi_{1n}(-h)\psi_{1n}(-h) & \dots & \psi_{1n}(-h)\psi_{mn}(-h) & \dots \\ \psi_{2n}(-h)\psi_{0n}(-h) & \psi_{2n}(-h)\psi_{1n}(-h) & \dots & \psi_{2n}(-h)\psi_{mn}(-h) & \dots \\ \vdots & \vdots & \vdots & \vdots & \vdots \\ \psi_{pn}(-h)\psi_{0n}(-h) & \psi_{pn}(-h)\psi_{1n}(-h) & \dots & \psi_{pn}(-h)\psi_{mn}(-h) & \dots \\ \vdots & \vdots & \vdots & \vdots & \vdots \end{pmatrix} \tag{4.69}$$

and

$$N_3 = \begin{pmatrix} 0 & 0 & 0 & \dots & 0 \\ 0 & \frac{\pi^2}{4h^2} & \vdots & \vdots & \vdots \\ 0 & 0 & \frac{2\pi^2}{4h^2} & \vdots & \vdots \\ \vdots & \vdots & \vdots & \vdots & \vdots \\ 0 & 0 & 0 & \frac{m^2\pi^2}{4h^2} & \vdots \\ \vdots & \vdots & \vdots & \vdots & \vdots \end{pmatrix}. \tag{4.70}$$

Therefore, in matrix form (4.65) can be written as

$$\xi N_1 \boldsymbol{A} + \xi N_2 \boldsymbol{A} - N_3 \boldsymbol{A} + \gamma_n^2 I \boldsymbol{A} = 0, \tag{4.71}$$

since $\gamma_n^2 = k^2 - s_n^2$ or

$$s_n^2 \boldsymbol{A} = N \boldsymbol{A} \tag{4.72}$$

where $N = (k^2 - N_3 + \xi N_1 + \xi N_2)$. The above equation (4.72) shows that s_n^2 are the eigenvalues of matrix N. These eigenvalues and the corresponding eigenvector can be computed numerically through some software. Let we write the eigenvector of (4.72) as X, then the field potential of liner region can be defined as

$$\boldsymbol{\phi}_2 = \boldsymbol{\psi}^t X D_2(x) \boldsymbol{A}_2 + \boldsymbol{\psi}^t X D_2(-x - L) \boldsymbol{B}_2 \tag{4.73}$$

where

$$D_2(x) = \begin{pmatrix} e^{is_0 x} & 0 & 0 & \dots & 0 & \dots \\ 0 & e^{is_1 x} & 0 & \dots & 0 & \dots \\ \vdots & \vdots & e^{is_2 x} & 0 & 0 & \dots \\ \vdots & \vdots & \vdots & \vdots & \vdots & \vdots \\ 0 & 0 & 0 & 0 & e^{is_n x} & \dots \\ \vdots & \vdots & \vdots & \vdots & \vdots & \vdots \end{pmatrix} \tag{4.74}$$

and

$$\boldsymbol{A}_2^t = \begin{bmatrix} A_0 & A_1 & \dots & A_n & \dots \end{bmatrix}, \tag{4.75}$$

$$\boldsymbol{B}_2^t = \begin{bmatrix} B_0 & B_1 & \dots & B_n & \dots \end{bmatrix}. \tag{4.76}$$

On differentiating (4.73) with respect to x

$$\frac{\partial \boldsymbol{\phi}_2}{\partial x} = \boldsymbol{\psi}^t X \frac{d}{dx} D_2(x) \boldsymbol{A}_2 + \boldsymbol{\psi}^t X \frac{d}{dx} D_2(-x - L) \boldsymbol{B}_2. \tag{4.77}$$

Now the field potential in duct regions can be written as follows

$$\boldsymbol{\phi}_1 = \boldsymbol{\psi}^t \left[D_1(x) \boldsymbol{A}_1 + D_1(-x) \boldsymbol{B}_1 \right], \tag{4.78}$$

$$\boldsymbol{\phi}_2 = \boldsymbol{\psi}^t \left[X D_2(x) \boldsymbol{A}_2 + X D_2(-x - L) \boldsymbol{B}_2 \right], \tag{4.79}$$

$$\boldsymbol{\phi}_3 = \boldsymbol{\psi}^t \left[D_1(x - L) \boldsymbol{A}_3 + D_1(L - x) \boldsymbol{B}_3 \right]. \tag{4.80}$$

Note that $\{A_1, A_2, A_3\}$ and $\{B_1, B_2, B_3\}$ are unknowns. We assume $\boldsymbol{B}_3 = 0$ and calculate rest of the unknowns through matching the pressure and normal velocities at interfaces $x = 0$ and $x = L$.

The continuity of pressure at $x = 0$ and $x = L$ is defined as

$$\phi_1(0, y) = \phi_2(0, y) \quad -h \leq y \leq h, \tag{4.81}$$

$$\phi_2(L, y) = \phi_3(L, y) \quad -h \leq y \leq h. \tag{4.82}$$

Likewise the continuity of normal velocities at $x = 0$ and $x = L$ can be given as

$$\frac{\partial}{\partial x}\phi_1(0, y) = \frac{\partial}{\partial x}\phi_2(0, y) \quad -h \leq y \leq h, \tag{4.83}$$

$$\frac{\partial}{\partial x}\phi_2(L, y) = \frac{\partial}{\partial x}\phi_3(L, y) \quad -h \leq y \leq h. \tag{4.84}$$

On using (4.78)-(4.80) into (4.81)-(4.84), we will obtain

$$\boldsymbol{\psi}^t \left[D_1(0)\boldsymbol{A}_1 + D_1(0)\boldsymbol{B}_1\right] = \boldsymbol{\psi}^t \left[X D_2(0)\boldsymbol{A}_2 + D_2(L)\boldsymbol{B}_2\right], \tag{4.85}$$

$$\boldsymbol{\psi}^t \left[X D_2(L)\boldsymbol{A}_2 + X D_2(0)\boldsymbol{B}_2\right] = \boldsymbol{\psi}^t \left[D_1(0)\boldsymbol{A}_3 + D_1(0)\boldsymbol{B}_3\right], \tag{4.86}$$

$$\boldsymbol{\psi}^t \left[D_1(0)k_R\boldsymbol{A}_1 - D_1(0)k_R\boldsymbol{B}_1\right] = \boldsymbol{\psi}^t \left[X k_Y D_2(0)\boldsymbol{A}_2 - D_2(L)k_Y\boldsymbol{B}_2\right], \tag{4.87}$$

$$\boldsymbol{\psi}^t \left[X k_Y D_2(L)\boldsymbol{A}_2 - X k_Y D_2(0)\boldsymbol{B}_2\right] = \boldsymbol{\psi}^t \left[D_1(0)k_R\boldsymbol{A}_3 - D_1(0)k_R\boldsymbol{B}_3\right]. \tag{4.88}$$

Multiplying $\boldsymbol{\psi}$ from (4.85)-(4.88) and integrate over $y = -h$ to $y = h$ to obtain the following equations

$$\boldsymbol{A}_1 + \boldsymbol{B}_1 = X(\boldsymbol{A}_2 + D_2(L)\boldsymbol{B}_2) \tag{4.89}$$

$$K_R(\boldsymbol{A}_1 - \boldsymbol{B}_1) = X K_y(\boldsymbol{A}_2 - D_2(L)\boldsymbol{B}_2) \tag{4.90}$$

$$\boldsymbol{A}_3 + \boldsymbol{B}_3 = X(D_2(L)\boldsymbol{A}_2 + \boldsymbol{B}_2) \tag{4.91}$$

$$K_R(\boldsymbol{A}_3 - \boldsymbol{B}_3) = X K_y(D_2(L)\boldsymbol{A}_2 - \boldsymbol{B}_2) \tag{4.92}$$

where K_R and K_Y are diagonal matrices containing the elements of axial wavenumber respectively,

$$K_R = \begin{pmatrix} \eta_0 & 0 & 0 & \ldots & 0 & \ldots \\ 0 & \eta_1 & 0 & \ldots & 0 & \ldots \\ \vdots & \vdots & \eta_2 & 0 & 0 & \ldots \\ \vdots & \vdots & \vdots & \vdots & \vdots & \vdots \\ 0 & 0 & 0 & 0 & \eta_n & \ldots \\ \vdots & \vdots & \vdots & \vdots & \vdots & \vdots \end{pmatrix} \tag{4.93}$$

and

$$K_Y = \begin{pmatrix} s_0 & 0 & 0 & \ldots & 0 & \ldots \\ 0 & s_1 & 0 & \ldots & 0 & \ldots \\ \vdots & \vdots & s_2 & 0 & 0 & \ldots \\ \vdots & \vdots & \vdots & \vdots & \vdots & \vdots \\ 0 & 0 & 0 & 0 & s_n & \ldots \\ \vdots & \vdots & \vdots & \vdots & \vdots & \vdots \end{pmatrix}. \tag{4.94}$$

Considering $\boldsymbol{B}_3 = 0$, then comparing (4.91) and (4.92), implies that

$$X D_2(L)(\boldsymbol{A}_2 + \boldsymbol{B}_2) = K_R^{-1} X K_y (D_2(L)\boldsymbol{A}_2 - \boldsymbol{B}_2) \tag{4.95}$$

or

$$(X - K_R^{-1} X K_y) D_2(L)\boldsymbol{A}_2 + (X + K_R^{-1} X K_y) D_2(L)\boldsymbol{B}_2 = 0. \tag{4.96}$$

We denote

$$F = X + K_R^{-1} X K_y \tag{4.97}$$

and

$$G = X - K_R^{-1} X K_y \tag{4.98}$$

implies that

$$\boldsymbol{B}_2 = -F^{-1} G D_2(L)\boldsymbol{A}_2. \tag{4.99}$$

Adding (4.91) and (4.92)

$$2\boldsymbol{A}_3 = FD_2(L)\boldsymbol{A}_2 + G\boldsymbol{B}_2. \tag{4.100}$$

On using (4.99) into (4.100)

$$2\boldsymbol{A}_3 = (FD_2(L) - GF^{-1}GD_2(L))\boldsymbol{A}_2. \tag{4.101}$$

Now adding (4.89) and (4.90)

$$2\boldsymbol{A}_1 = F\boldsymbol{A}_2 + GD_2(L)\boldsymbol{B}_2, \tag{4.102}$$

using value of $\boldsymbol{B}_2$, we will get

$$2\boldsymbol{A}_1 = (F - GD_2(L)F^{-1}GD_2(L))\boldsymbol{A}_2. \tag{4.103}$$

Subtracting (4.89) and (4.90)

$$2\boldsymbol{B}_1 = (G - FD_2(L)F^{-1}GD_2(L))\boldsymbol{A}_2. \tag{4.104}$$

Now to obtain the reflection and transmission coefficients by

$$T(t) = A_3 A_1{}^{-1} \quad \text{and} \quad R(r) = B_1 A_1{}^{-1}, \tag{4.105}$$

implies that

$$T(t) = (FD_2(L) - GF^{-1}GD_2(L))(F - GD_2(L)F^{-1}GD_2(L))^{-1} \tag{4.106}$$

and

$$R(r) = (G - FD_2(L)F^{-1}GD_2(L))(F - GD_2(L)F^{-1}GD_2(L))^{-1}. \tag{4.107}$$

4.3   Numerical Results

In this section the numerical results are presented. The problem is excited with the fundamental duct mode of inlet region that scatters on interaction with the lined chamber. The fundamental reflected mode in inlet and the fundamental transmitted mode in outlet are plotted against frequency. These modes carry maximum of the incident energy. For numerical computation the dimensional heights of inlet/outlet $h = 0.05m$ and length of the chamber $l = 0.1m$ are taken whilst the depth of the liner $b - h$ is assumed different by considering $b = 0.1m$, $0.2m$ and $0.3m$. The speed of sound $c = 343.5\text{m/s}$ and $k = 2\pi f/c$, where f is frequency measured in Hertz. For $b = 0.1m$ the absolute value of fundamental reflected mode in inlet $|R_0|$ and the absolute value of transmitted mode in outlet $|T_0|$ plotted against frequency f (Hz) are shown in Fig. 4.3 and Fig. 4.4, respectively.
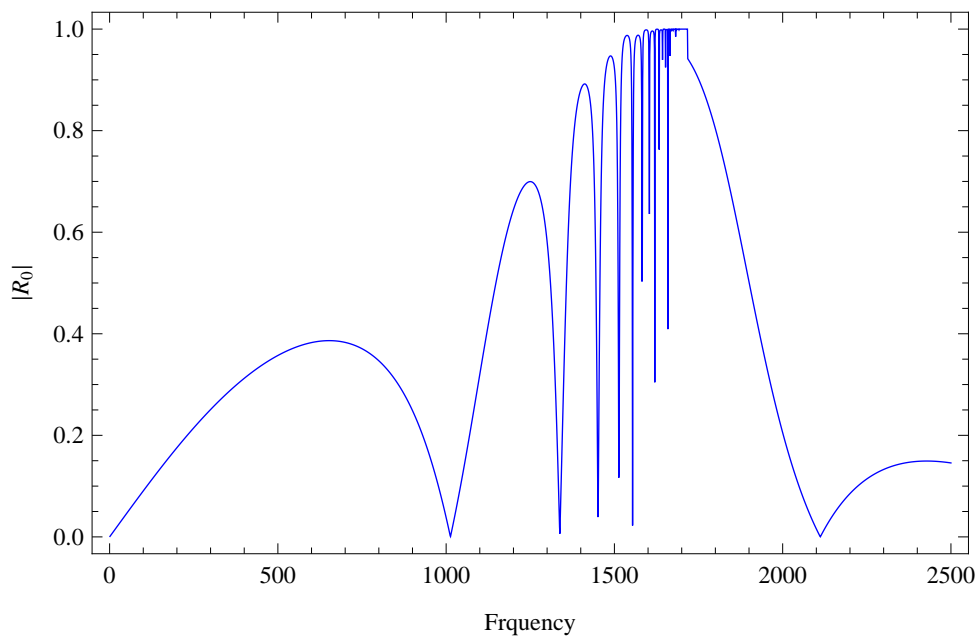
Figure 4.3: The absolute fundamental reflected mode against frequency for $b = 0.1m$, where $h = 0.05m$ and $l = 0.1m$

From Fig. 4.3 it can be seen that in start reflected amplitude is minimum which vary on increasing frequency and the reaches to its maximum value about frequency regime $1400Hz \leq f \leq 1700Hz$ whereas transmitted amplitude behave inversely (see Fig. 4.4).
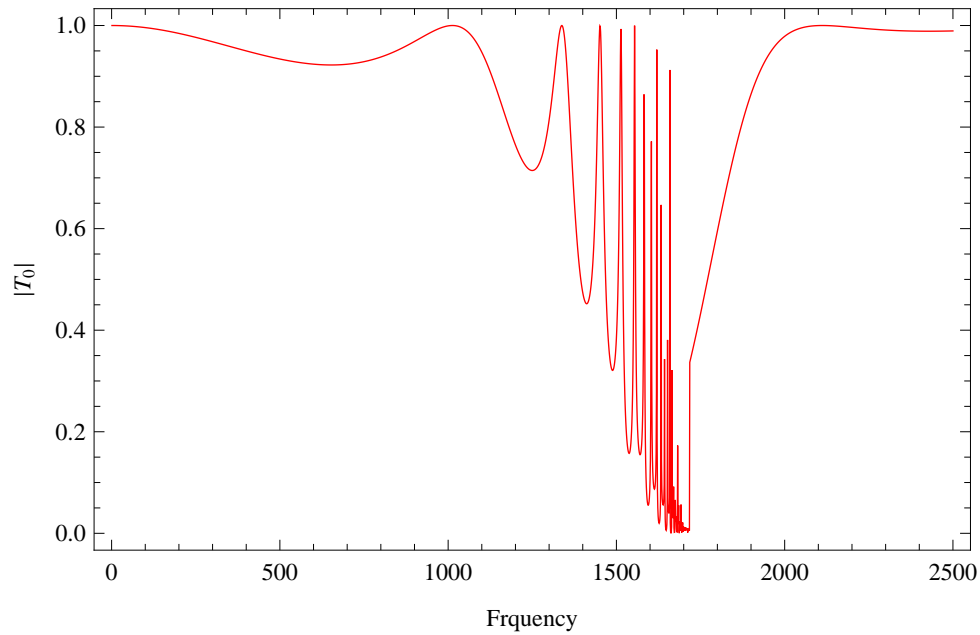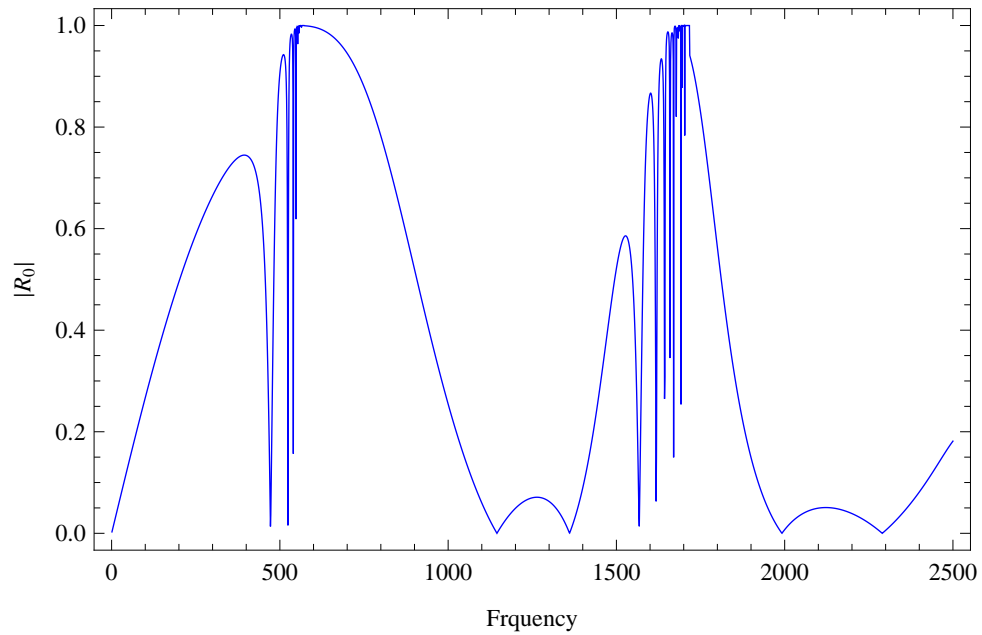
Figure 4.4: The absolute fundamental transmitted mode against frequency for $b = 0.1m$, where $h = 0.05m$ and $l = 0.1m$

This variation is because of the occurrence of new propagating modes in the duct regions and the change of eigenvalues from imaginary number to real number or complex and vice versa.

Likewise for $b = 0.2$ the absolute value of fundamental reflected mode and the absolute value of transmitted mode are shown in Fig. 4.5 and Fig. 4.6, respectively. Accordingly, for $b = 0.3$ the absolute value of fundamental reflected mode and the absolute value of transmitted mode are shown in Fig. 4.7 and Fig. 4.8, respectively. From these graphs it is found that by increasing the depth of liner cavities different narrow bands occur in chosen frequency domain instead of a single wider band as revealed in Figs. 4.3 and 4.4.

Figure 4.5: The absolute fundamental reflected mode against frequency for $b = 0.2m$, where $h = 0.05m$ and $l = 0.1m$.
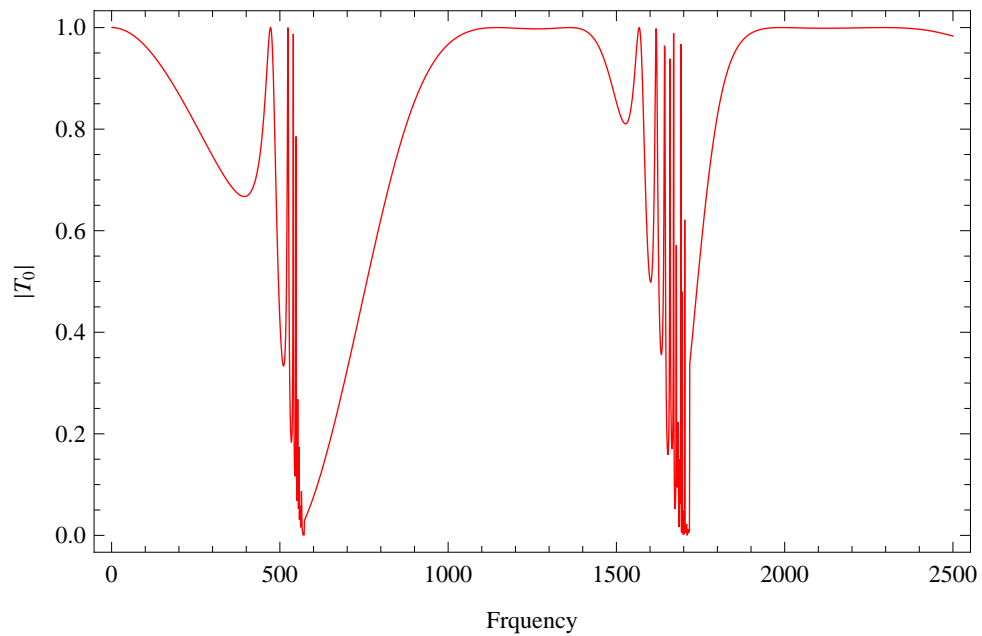

Figure 4.6: The absolute fundamental transmitted mode against frequency for $b = 0.2m$, where $h = 0.05m$ and $l = 0.1m$.
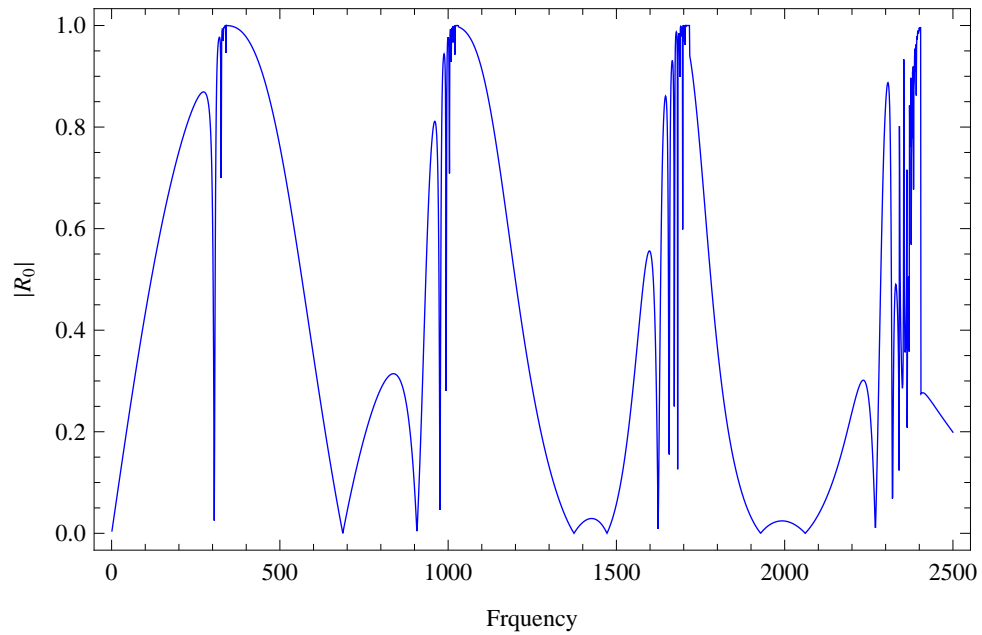
Figure 4.7: The absolute fundamental reflected mode against frequency for $b = 0.3m$, where $h = 0.05m$ and $l = 0.1m$.
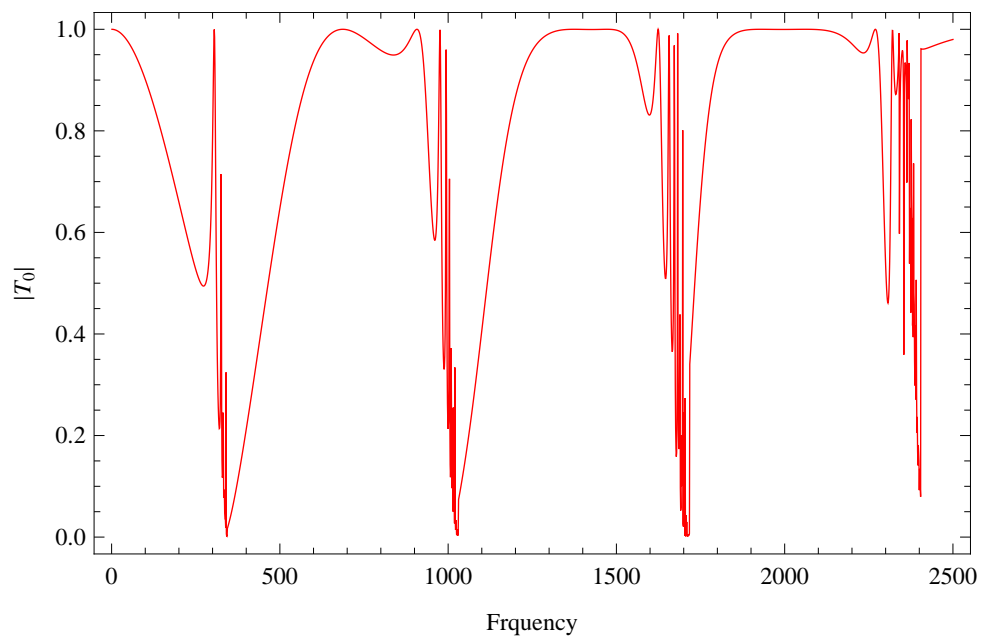

Figure 4.8: The absolute fundamental transmitted mode against frequency for $b = 0.3m$, where $h = 0.05m$ and $l = 0.1m$.

Thus, the depth of the cavity affect significantly the scattering energies and by changing the depth the devise can be made more operative. In Figs. 4.9-4.10 and Figs. 4.11-4.12, the absolute value of fundamental reflected mode and the absolute value of transmitted mode are shown by taking length of the cavities $l = 0.2m$

and $l = 0.3m$, respectively, whereas $h = 0.05m$ and $b = 0.1m$. It can be seen that by changing the length of the chamber cavities the a variation in scattering amplitudes is revealed.
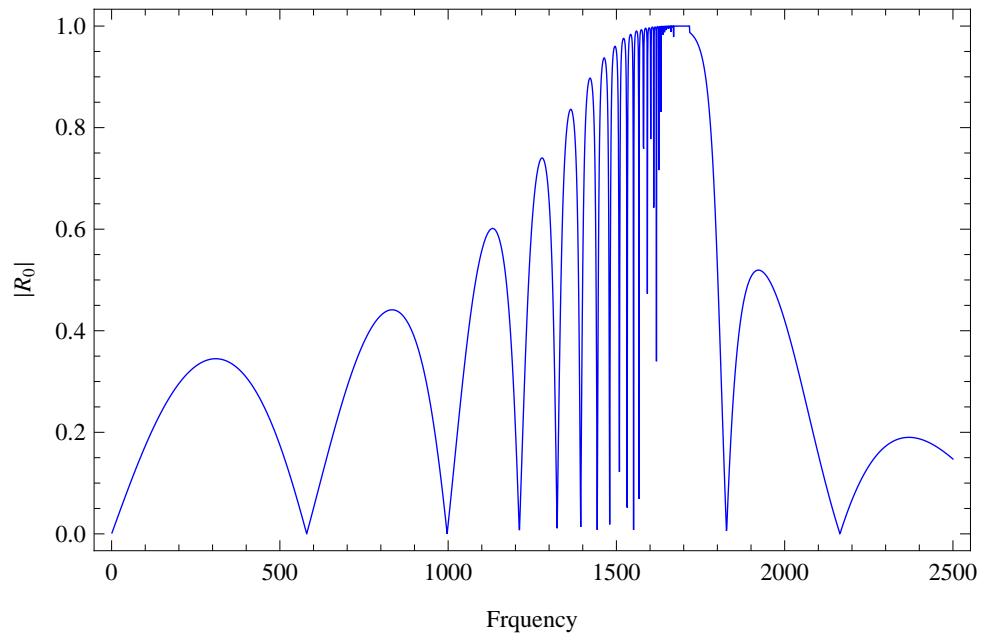

Figure 4.9: The absolute fundamental reflected mode against frequency for $l = 0.2m$, where $h = 0.05m$ and $b = 0.1m$.
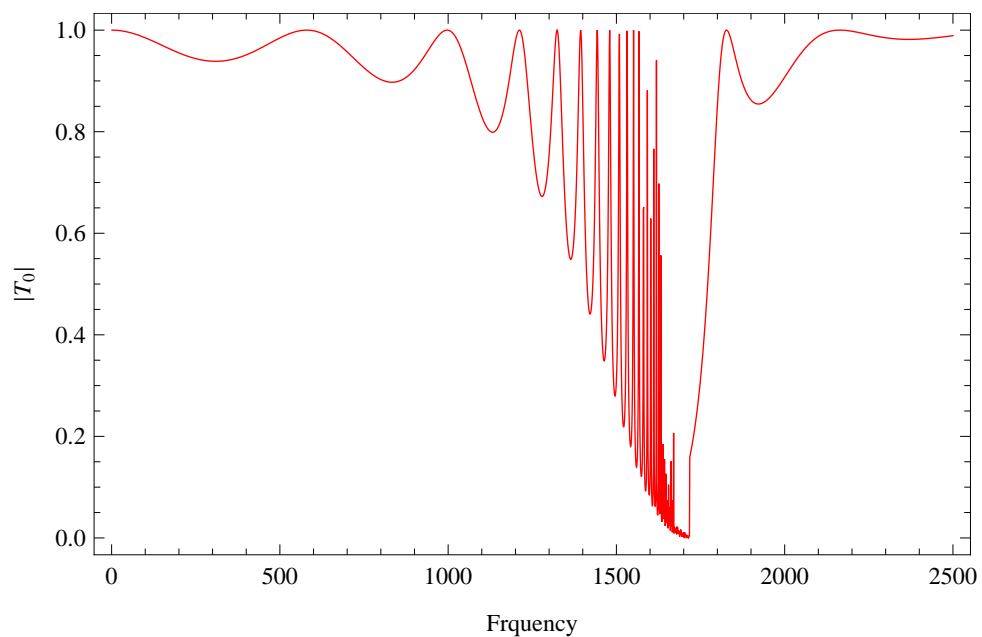

Figure 4.10: The absolute fundamental transmitted mode against frequency for $l = 0.2m$, where $h = 0.05m$ and $b = 0.1m$.
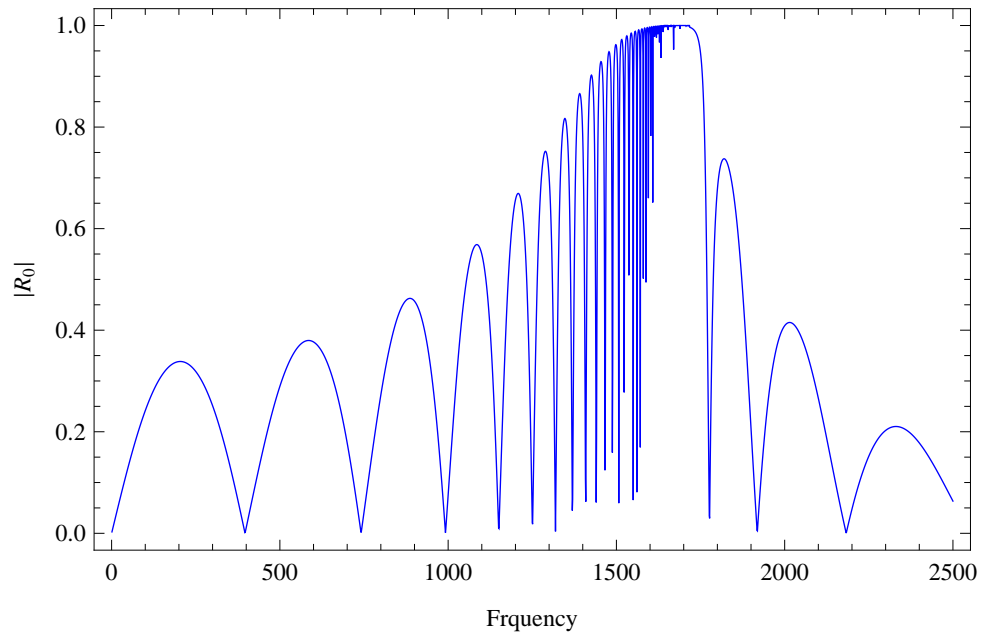
Figure 4.11: The absolute fundamental reflected mode against frequency for $l = 0.3m$, where $h = 0.05m$ and $b = 0.1m$.
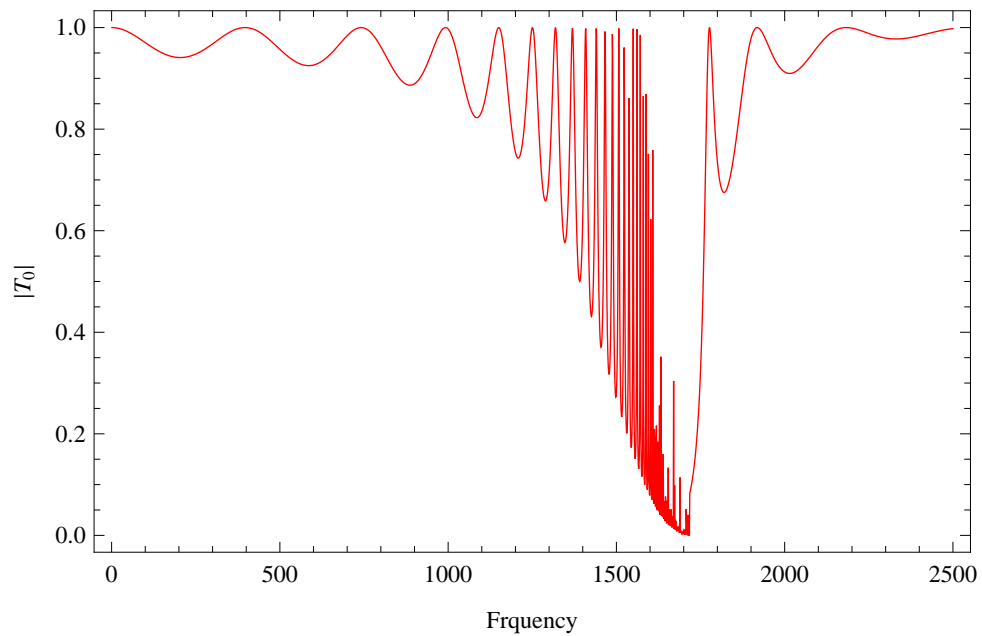

Figure 4.12: The absolute fundamental transmitted mode against frequency for $l = 0.3m$, where $h = 0.05m$ and $b = 0.1m$.

Chapter 5

Discussion and Conclusion

The work presented in this thesis explore the Multi-Modal solution of the physical problem containing lined expansion chamber. The solution is sorted first for two prototype problems exited by the plane pistons lying along the wall of duct. The first problem is bounded by rigid walls whilst the second problem comprises linings along the horizontal wall. These problems are governed with Helmholtz's equation and contain boundary conditions to be rigid-rigid and rigid-impedance. The formulation of the envisaged boundary value problems and their solutions are discussed in Chapter-3 of the thesis. Both of these problems are solved with the Multi-modal and Mode-matching methods. The numerical results are presented to show the effects of the velocity of the piston on scattering amplitudes. From these results it is found that by changing the velocity of the moving piston a variation in scattering of fundamental and secondary mode is obtained. Moreover, an excellent agreement between Multi-modal and Mode-Matching solution is achieved.

Whereas, in Chapter-4 the scattering from an expansion chamber including two cavity regions is discussed. The mathematical modeling of the liner cavity is explained. Then a physical problem containing an expansion chamber having two liner cavities is modeled to analyze the acoustic scattering. The governing boundary value problem is solved by using the Multi-modal method. For different values of depth and width parameters of the chamber, the reflected and transmitted mode amplitudes are plotted against frequency. From the numerical result, it is found

that by changing the depth and width of the liner cavities a variation in passing and stopping bands is found. This makes the device more operative for certain frequency regimes.

Bibliography

[1] R. Mangiarotty, Acoustic-lining concepts and materials for engine ducts, The Journal of the Acoustical Society of America, 48(3C): 783-794 (1970).

[2] W. Bi, V. Pagneux, D. Lafarge and Y. Auregan, Sound propagation in non-uniform lined duct by the multimodal method, Proceeding of 10th International Conference on Sound and Vibration, 3229-3236 (2003).

[3] J. Allard and N. Atalla, Propagation of sound in porous media: modelling sound absorbing materials, John Wiley and Sons (2009).

[4] K. Peat, The acoustical impedance at the junction of an extended inlet or outlet duct, Journal of Sound and Vibration, 150(1): 101-110 (1991).

[5] B. Regan and J. Eaton, Modelling the influence of acoustic liner non-uniformities on duct modes, Journal of Sound and Vibration, 219(5): 859-879 (1999).

[6] T. Elandy, H. Boden and R. Glav, Application of the point matching method to model circumferentially segmented non-locally reacting liners, 7th AIAA/CEAS Aeroacoustics Conference and Exhibit, 2202 (2001).

[7] S. Felix and V. Pagneux, Sound propagation in rigid bends: A multimodal approach, The Journal of the Acoustical Society of America, 110(3): 1329-1337 (2001).

[8] W. Bi, V. Pagneux, D. Lafarge and Y. Auregan, Modelling of sound propagation in a non-uniform lined duct using a multi-modal propagation method, Journal of Sound and Vibration, 289(4-5): 1091-1111 (2006).

[9] R. Kirby, P. Williams and J. Hill, A comparison between the performance of different silencer designs for gas turbine exhaust systems, (2012).

[10] J. B. Lawrie, Analytic mode-matching for acoustic scattering in three dimensional waveguides with flexible walls: Application to a triangular duct, Wave Motion, 50(3): 542-557 (2013).

[11] R. Nawaz and J. B. Lawrie, Scattering of a fluid-structure coupled wave at a flanged junction between two flexible waveguides, The Journal of the Acoustic Society of America, 134(3): 1939-1949 (2013).

[12] M. Afzal, R. Nawaz, M. Ayub and A. Wahab, Acoustic scattering in flexible waveguide involving step discontinuity, 9(8): (2014).

[13] R. Nawaz, M. Afzal and M. Ayub, Acoustic propagation in two dimensional waveguide for membrane bounded ducts, Communications in Nonlinear Science and Numerical Simulation, 20(2): 421-433 (2015).

[14] M. H. Meylan and A. Bashir, Mode matching analysis for wave scattering in triple and pentafurcated spaced ducts, Mathematical Methods in the Applied Sciences, 39(11): 3043-3057 (2016).

[15] M. Afzal, M. Ayub, R. Nawaz and A. Wahab, Mode-matching solution of a scattering problem in flexible waveguide with abrupt geometric changes, Multiscale and High Contrast Partial Differential Equations, 660: 113-29 (2016).

[16] M. Afzal, R. Nawaz and A. Ullah, Attenuation of dissipative device involving coupled wave scattering and change in material properties, Applied Mathematics and Computation, 290: 154-163 (2016).

[17] S. Shafique, M. Afzal and R. Nawaz, On mode-matching analysis of fluid structure coupled wave scattering between two flexible waveguides, Canadian Journal of Physics, 95(6): 581-589 (2017).

[18] M. Afzal and J. Lawrie, Acoustic scattering in a waveguide with a height discontinuity bridged by a membrane, Journal of Engineering and Applied Mathematics, 105(1): 99-115 (2017).

[19] T. Nawaz, M. Afzal and R. Nawaz, The scattering analysis of trifurcated waveguide involving structural discontinuities, Advance in Mechanical Engineering, 11(7): (2019).

[20] J. U. Satti, M. Afzal and R. Nawaz, Scattering analysis of a partitioned wave-bearing cavity containing different material properties, Physica Scripta, 94(11): 115223 (2019).